REGULATION OF STRIATED MUSCLE METABOLISM AND FUNCTION BY MEDIATOR COMPLEX

APPROVED BY SUPERVISORY COMMITTEE

Eric N. Olson, Ph.D.

Steven A. Kliewer, Ph.D.

James T. Stull, Ph.D.

Ondine Cleaver, Ph.D.

Dedicated to my parents

REGULATION OF STRIATED MUSCLE METABOLSIM AND FUNCTION BY MEDIATOR COMPLEX

by

SUSAN M. DELEON

DISSERTATION

Presented to the Faculty of the Graduate School of Biomedical Sciences

The University of Texas Southwestern Medical Center at Dallas

In Partial Fulfillment of the Requirements

For the Degree of

DOCTOR OF PHILOSOPHY

The University of Texas Southwestern Medical Center at Dallas

Dallas, Texas

August, 2015

REGULATION OF STRIATED MUSCLE METABOLSIM AND FUNCTION BY MEDIATOR COMPLEX

SUSAN M. DELEON, Ph.D.

The University of Texas Southwestern Medical Center at Dallas, 2015

Supervising Professor: Eric N. Olson, Ph.D.

Mediator is a multi-protein complex that links signal-dependent transcription factors and upstream regulators with polymerase II (Pol II) to form a stable and efficient pre-initiation complex (PIC). Recent studies have suggested that different compositions of subunits in Mediator in a cell-specific and signal-dependant manner, which permits customizable regulation of different subsets of genes, and variable responses to signals from transcription factors. In this way, Mediator allows for response to the continuous changes of the cellular environment. Our studies have implicated the mediator subunit

MED13 in the control of cardiac and skeletal muscle metabolism. MED13, along with MED12, cyclin C and cdc8, form the kinase module of the Mediator complex, which is thought to function as an accessory repressor or activator of Mediator. To investigate the potential role of MED12 in striated muscle functions, we generated mice with conditional deletion of MED12 in the heart and skeletal muscle. Mice with cardiac deletion of MED12 display postnatal cardiomyopathy with dysregulation of genes involved in calcium homeostasis and contractility. Mice with skeletal muscle deletion of MED12 show severe muscle defects and a failure to thrive, which likely reflects a role of this Mediator subunit in the control of muscle growth. Collectively, these highlight distinct roles of the kinase module of the Mediator complex in cardiac and skeletal muscle development and function.

TABLE OF CONTENTS

PRIOR PUBLICATIONS

Caldwell, K.A., Tucci, M.L., Armagost, J., Hodges, T.W., Chen, J., Memon, S.B., Blalock, J.E., **DeLeon, S.M.**, Findlay, R.H., Ruan, Q., Webber, P.J., Standaert, D.G., Olson, J.B., Caldwell, G.A. (2009). Investigating bacterial sources of toxicity as an environmental contributor to dopaminergic neurodegeneration. PLoS One. 4(10):e7227.

Grueter, C.E., van Rooj, E., Johnson, B.A., **DeLeon, S.M.**, Sutherland, L.B., Qi, X., Gautron, L., Elmquist, J.K., Bassel-Duby, R., Olson, E.N. (2012). A cardiac microRNA governs systemic homeostasis by regulation of MED13. Cell. 149(3), 671-683.

Knight, A.L., Yan, X., Hamamichi, S., Ajjuri, R.R., Mazzulli, J.R., Zhang, M.W., Daigle, J.G., Zhang, S., Borom, A.R., Roberts, L.R., Lee, S.K., **DeLeon, S.M.**, Viollet-Djelassi, C., Krainc, D., O'Donnell, J.M., Caldwell, K.A., Caldwell, G.A. (2014). The glycolytic enzyme, GPI, is a functionally conserved modifier of dopaminergic neurodegeneration in Parkinson's models. Cell Metabolism. 20(1):145-57./

LIST OF FIGURES

LIST OF TABLES

LIST OF APPENDICES

LIST OF ABREVIATIONS

αMHC/aMHC – myosin heavy chain, alpha

βMHC/bMHC – myosin heavy chain, beta

CDK – Cyclin-dependent kinase

cKO – cardiac-specific knockout (αMHC-Cre)

CTL – control (Med12 fl/Y)

DCM – dilated cardiomyopathy

EDL – extensor digitorum longus

Fl – floxed (flanked by loxP sites)

FS – fractional shortening

HF – heart failure

HFD – high-fat diet

LNA – locked nucleic acid

MCK – muscle creatine kinase

MEF2 – myocyte enhancer factor 2

miR – microRNA

MyoD – myogenic differentiation 1

NR – nuclear receptor

LVIDd – left ventricular internal diameter (diastole)

LVIDs – left ventricular internal diameter (systole)

Pol II – RNA polymerase II

mKO – skeletal muscle-specific knockout (myogenin-Cre)

SERCA – sarcoplasmic reticulum Ca^{2+}-ATPase

SOL – soleus

SR – sarcoplasmic reticulum

SRF – serum response factor

TA – tibialis anterior

TG – transgenic (over-expression)

TGA – transposition of the great arteries

TH – thyroid hormone

TR – thyroid-hormone receptor

WT – wild-type

CHAPTER I

STRIATED MUSCLE DEVELOPMENT AND FUNCTION

Introduction

Multiple transcriptional pathways have been implicated in the complex regulation of basal cardiac and skeletal muscle fiber type specific gene expression, stress induced remodeling, and myocyte metabolism. During muscle sarcomere contraction, actin thin filaments slide towards myosin thick filaments and the two proteins form cross-bridges in an ATP-dependent manner. The mechanism by which contractile and calcium regulatory genes are concordantly regulated to produce a unified effect on muscle contraction is currently poorly understood. In this chapter, discussion will be centered on the transcriptional pathways that govern cardiac and skeletal muscle contractility, as well metabolic function.

The Sarcomere and Striated Muscle Contractility

The striated appearance of cardiac and skeletal muscle arises from the repeating arrangement of individual contractile units called sarcomeres. Each sarcomere is highly organized, composed of thick filaments intercalated between Z-disk-bound thin filaments

(Figure 1.1). According to the sliding filament theory, first published in 1954, sarcomeric contraction occurs when thick filament myosins bind to actin thin filaments, and hydrolyze ATP to generate a power stroke (Spudich, 2001). This process is tightly regulated by the calcium sensitive troponin/tropomyosin complex, which modifies its conformation to allow actin-myosin interactions in response to increased intracellular calcium following membrane depolarization (Lehman et al., 1994).

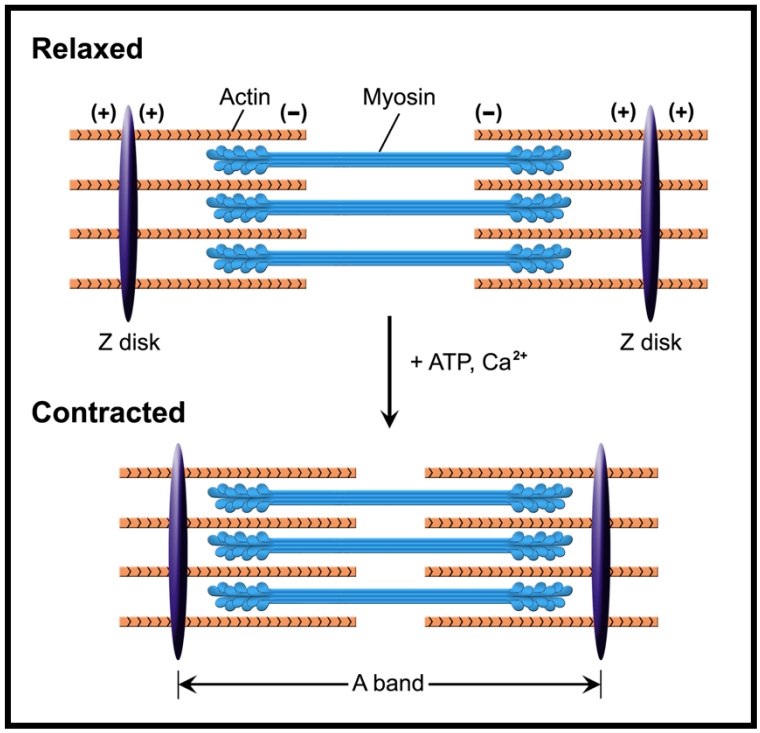

Figure 1.1 Striated muscle sarcomere contraction in response to intracellular calcium.

In cardiac tissue, membrane depolarization begins in the pacemaker cells in the sinoatrial node, which is innervated by both sympathetic and parasympathetic nerves. External stimuli cause the pacemaker cells to undergo spontaneous self-depolarization,

producing action potentials, via a slow leak of potassium ions and a simultaneous influx of sodium and calcium ions. The action potential then carries across to the cardiac myocytes, where it enters the T-tubules (invaginations of the membrane containing numerous ion channels). Within cardiomyocytes, the influx of calcium across the plasma membrane elicits calcium release from the sarcoplasmic reticulum (SR) via Ryanodine receptor (RyR) by calcium-induced calcium release (CICR) (Kuo and Ehrlich, 2015; Sanbe et al., 1999). Contraction in skeletal muscle occurs in a very similar manner (Figure 1.2).

In skeletal muscle, however, instead of CICR influencing calcium release from the SR, the L-type calcium channels are directly coupled to RyR proteins. Skeletal muscle membrane depolarization is initiated at the neuromuscular junctions (NMJs), where motor neurons innervate skeletal muscle. The motor neuron synapse signals to the muscle fiber through the release of acetylcholine across the synaptic cleft, where it binds to acetylcholine receptors (AChRs). Activation of the AChR leads to an influx of sodium and calcium ions, causing depolarization of the muscle cell membrane, and eliciting an action potential. As the action potential propagates and invades T-tubules, L-type voltage gated calcium channels lining the T-tubules undergo a conformational change, activating RyR1 on the closely apposed SR for calcium release (Figure 1.2) (Kuo and Ehrlich, 2015).

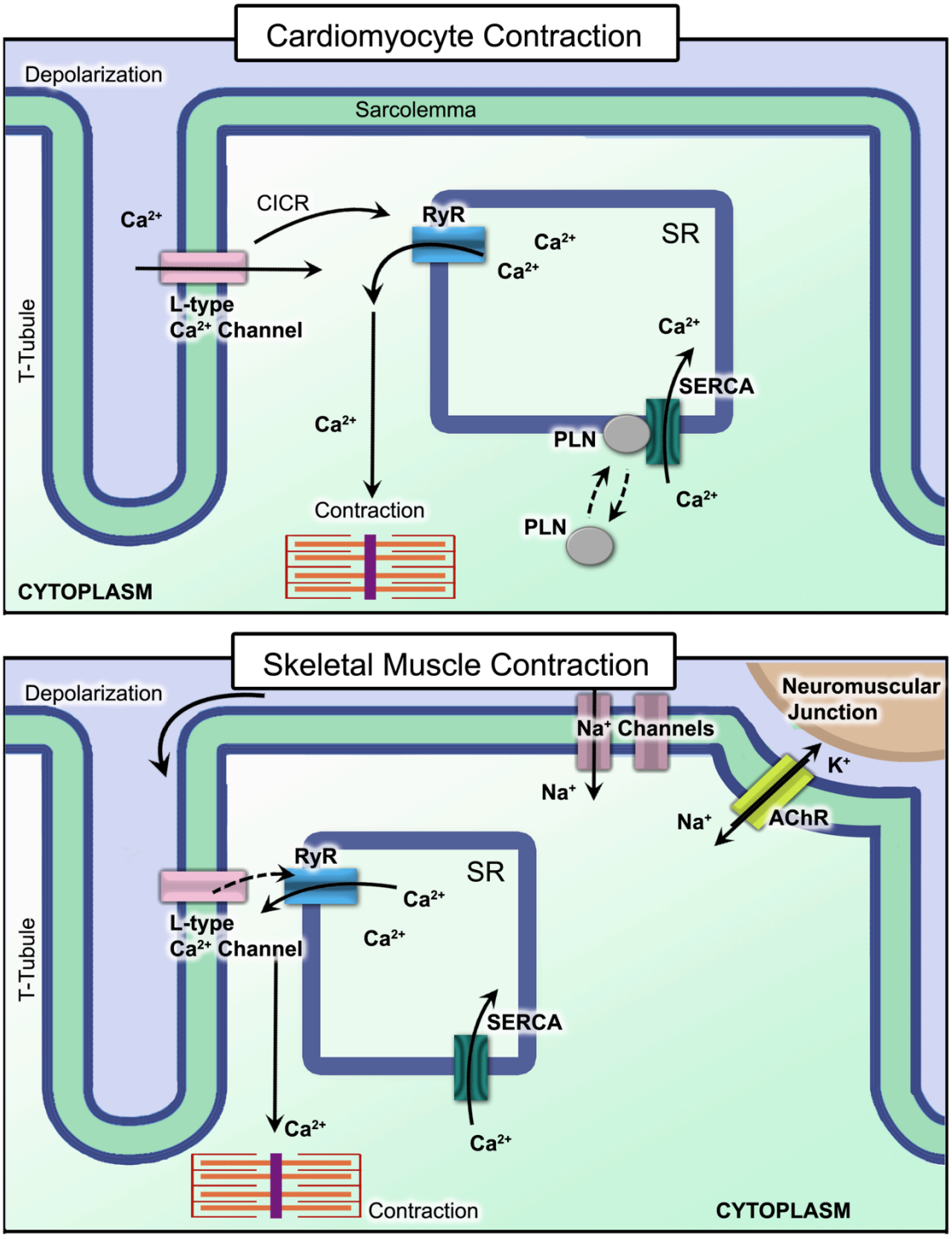

Figure 1.2 Contractility and calcium handling in striated muscle.

With skeletal muscle, multiple isoforms of contractile apparatus proteins are regulated in a fiber-type specific manner, and can profoundly influence overall muscle function (Bandman, 1992). Alternate combinations of troponin T, I, and C protein isoforms influence myofiber Ca^{2+} sensitivity in muscle, while differential expression of myosin heavy chain (Myh) isoforms can alter force-velocity ranges of individual muscle fibers (Bottinelli et al., 1991; Geiger et al., 1999).

The mechanism by which contractile and calcium regulatory genes are concomitantly regulated to produce a convergent effect on muscle contraction is not well understood. Beyond actin and myosin, there are a number of proteins that support the sarcomere and regulate striated muscle contraction, as well as those that affect metabolism and overall muscle function. Some of these proteins and the networks in which they act will be further discussed in this chapter.

Heart Disease, Muscle Function, and Metabolism

Cardiomyopathies

Hypertrophic cardiomyopathy (HCM) is a monogenic disease that can be caused by a mutation in 1 of 13 or more genes encoding protein components of the sarcomere, (Alcalai et al., 2008) and others in desmosomal proteins have been observed, as well (Hershberger et al., 2013). In the U.S. alone, the incidence of HCM is approximately 1 in 500, affecting an estimated 600,000 people nationally. This relatively high prevalence is also similarly seen in various other geographic locales (Maron et al., 1995). HCM is

characterized by its phenotypic presentation of thickening of the myocardium, particularly in the left ventricle (Figure 1.3). Cardiomyopathies can also manifest as dilation of the left ventricle, sometimes also affecting the right, and increasing end-diastolic dimension. This is referred to as dilated cardiomyopathy (DCM), and is estimated to affect 1 in 250-400 individuals. Almost all patients exhibit decreases in systolic function. In HCM, end-diastolic function of the left ventricle is decreased, and systolic function is either preserved or increased. Another distinct cardiomyopathy, referred to as arrhythmogenic right ventricular cardiomyopathy (ARVC), is characterized by replacement of the myocardium with adipocytes and fibrous deposits. This replacement typically and leads to right ventricular dilation, arrhythmia, ventricular failure, and sudden cardiac death (McRae et al., 2001). The general phenotypic distinction between HCM, DCM, and ARCV is well-established (Figure 1.3). However, for the purposes of this dissertation, DCM will be further expanded upon.

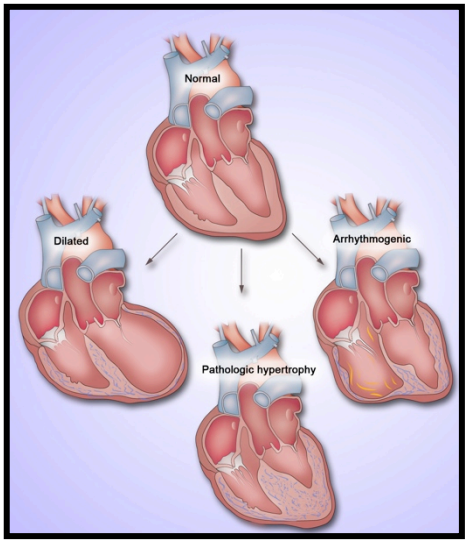

Figure 1.3. Differential morphology of various cardiomyopathies. Modified from (Hershberger et al., 2013).

Substantial genetic overlap exists between HCM and DCM, both of which have shown with incomplete penetrance and variable inter-individual phenotypic expression. However, in contrast to the gene families known to be responsible for HCM, which are associated with specific gene ontologies, the genetic basis for DCM is highly diverse. Approximately 40% of the genetic causes of DCM have been identified in mutations of over 30 genes, which affect the function of a diverse array of proteins (Hershberger et al., 2013).

Heart disease and aberrant cardiac metabolism

In addition to the various genetic causes of cardiomyopathy, obesity and type 2 diabetes are also associated with an increase in risk of developing heart disease. Visceral adiposity and insulin resistance can lead to dyslipidemia, hypertension, and glucose dysmetabolism (Van Gaal et al., 2006). As the heart adapts to changes in diet and stress through fine-tuning metabolism and gene expression patterns, it stands susceptible to impaired metabolism and ultimately heart failure (Balaban et al., 1986). Myocardial lipid accumulation is an early abnormality observed in obese and insulin-resistant individuals (Harmancey et al., 2008). Moreover, crosstalk between the heart and adipose tissue includes adipokines such as leptin and adiponectin secreted from the adipocytes, signaling to the heart and altering its genetic programming, potentially leading to increased oxidative stress and endothelial dysfunction (Van Gaal et al., 2006). Thus, it is also important to examine regulation of the cardiac transcriptional pathways, mechanisms of inter-tissue signaling, and the role of the cardiometabolic axis in disease.

The heart requires a continuous supply of ATP to sustain uninterrupted contractility and function. Under typical conditions, the heart derives the majority of its energy from mitochondrial oxidation of fatty acids. Myocardial function and metabolism is modulated in response to physiological, pathological and developmental conditions (Carvajal and Moreno-Sanchez, 2003). During the transition from embryonic to postnatal development, the heart shifts from glucose to fatty acids as the predominant energy source. Conversely, during pathological heart failure, mitochondrial oxidative capacity is diminished and the metabolism of the heart shifts away from fatty acids toward glycolytic metabolism. Genetic mutations that perturb fatty acid uptake or metabolism by the heart cause severe developmental abnormalities in humans (Carvajal and Moreno-Sanchez, 2003). Given the importance of cardiac metabolism for maintenance of cardiac energetics during homeostasis and disease, a deeper understanding of the molecular mechanisms that modulate energy usage during heart disease may provide new approaches to enhance cardiac function.

Transcriptional control of striated muscle metabolism and function

The heart adapts to changes in diet and stress by fine-tuning metabolic substrate utilization and gene expression patterns to maximize energy efficiency. Members of the nuclear receptor (NR) superfamily play an especially prominent role in the control of cardiac metabolism. NRs, along with their coactivators and corepressors, regulate cardiac metabolism at the transcriptional level through responding to, physiological and pathological cues (Huss and Kelly, 2004). PPARγ co-activator-1 (PGC-1) α and β are

preferentially expressed in tissues with high-capacity mitochondrial function such as the heart brown adipose tissue, and slow skeletal muscle (Finck and Kelly, 2006; Lin et al., 2005). These coactivators play critical roles in the control of energy metabolism by activating the expression of genes involved in mitochondrial biogenesis and respiratory function in conjunction with nuclear hormone receptors, including PPARs, RXRs, and estrogen-related receptors (ERRs), and the MEF2 transcription factor (Czubryt et al., 2003; Finck and Kelly, 2007; Lin et al., 2005). MEF2, in turn, regulates expression of PGC-1α, thereby establishing a transcriptional network to control energy metabolism. PGC-1α is the most well-studied of the PGC-1 genes, and also regulates muscle glucose uptake (Lin et al., 2002). Both PGC-1α and β control transcriptional programs required for the metabolic and functional maturation of the heart, and their targets are down-regulated in pathological forms of cardiac hypertrophy and heart failure (Arany et al., 2005; Leone et al., 2005; Lin et al., 2005). Conversely, these coactivators are up-regulated during postnatal growth or exercise training (Finck and Kelly, 2006; Rowe et al., 2010). Nuclear receptors, such as PPARs, ERRs, TRs, and Nur77 activate transcription of genes involved in myofiber switching. PGC-1α is a coregulator and acts with PPAR, ERR, and TR to drive the switch from fast to slow fibers (Baskin et al., 2014).

Thyroid Hormone Signaling

Cardiac metabolism is highly sensitive to thyroid hormone (TH) signaling. TH acts in transcriptional regulation by binding nuclear TH receptors (TRs) (Watanabe et al.,

2006). Depending on the transcriptional cofactors present, TH stimulates and represses TRs, eliciting positive and negative effects on transcription of TR-dependent genes. Activation of TRs through increased production of TH, as well as resistance to TH signaling, results in enhanced energy expenditure and a lean phenotype (Mitchell et al., 2010; Watanabe et al., 2006). Many metabolic genes targeted by TRs are known (Zhu and Cheng, 2010). However, much remains to be learned about the molecular pathways that regulate TH signaling and energy homeostasis in the heart.

Skeletal muscle is also a key target of TH signaling, and many patients of thyroid disorders often demonstrate myopathic symptoms. Thyroid hormone has emerged as a powerful regulator of muscle contractility and metabolic homeostasis. The concerted effects of TH signaling on both contractile and metabolic properties of muscle have revealed an exceptionally complex interplay of direct and indirect mechanisms, dependent on tissue-specific modulation of intracellular TH levels or on circulating TH levels. [Table 1.1]. The regulation of the proteins listed in Table 1.1 is also congruent with the TH-induced increase in both glycolytic and oxidative capacities (Salvatore et al., 2014).

Table 1.1. Effects of thyroid hormone signaling on skeletal muscle properties

Muscle Function	TH-Regulated Proteins	Associated effect
Contractility	MYH7, MYH1, MYH2, MYH4	Increased rate of contraction
	SERCA1a, SERCA2a	Increased rate of relaxation
Metabolism	NA+/K+ ATPase, SERCA1a, SERCA2a	Decreased energetic efficiency of contraction due to higher ATP consumption associated with fluxes of NA+/K+ and Ca2+ at rest and during activity
	GLUT-4, ME1	Increased glycolytic capacity leading to increased ATP generation
	PGC-1α	Increased mitochondrial density leading to increased ATP generation
	UCP3, mGPH	Decreased mitochondrial efficiency

Source: Salvatore et al., Nature Endocrinology, 2014

Calcium-induced signaling

Chronic muscle stimulation induces a reversible transition in myofiber phenotype from fast to slow, suggesting physical conditions that lead to alterations in the frequency of muscle stimulation affect muscle fiber type (Pette and Staron, 1997). This is further supported by studies showing decreased muscle usage results in a loss of slow myofibers, while endurance exercise results in the conversion of fast myofibers towards a slow, fatigue resistant phenotype (Allen et al., 2001; Templeton et al., 1988). Persistent muscle stimulation results in increased calcium transients, which activate the calcium-sensitive signaling serine/threonine phosphatase calcineurin. Calcineurin, in turn, dephosphorylates the transcription factor NFAT, Nuclear factor of activated T cells, to induce nuclear shuttling from the cytoplasm, allowing NFAT to transactivate target genes in the nucleus (Crabtree and Olson, 2002). Transgenic over-expression of activated calcineurin in

skeletal muscle was sufficient to induce conversion of myofibers from fast to slow, recapitulating the phenotype that occurs following an increase in calcium transients (Naya et al., 2000).

Serum Response Factor

Several cardiac specific Serum response factor (SRF) knockouts have been characterized to date. Deletion of SRF in the embryonic heart using βMHC-Cre transgenic mice impairs cardiac differentiation and maturation and disrupts the expression of multiple regulators of cardiac development, such as Nkx2.5 and GATA4, resulting in embryonic lethality between E10.5 and E13.5 (Parlakian et al., 2004). Ablation of SRF using αMHC-Cre mice results in cardiac insufficiency and reduced cellularity during cardiogenesis accompanied by reductions in cardiac, skeletal, and smooth muscle α-actin transcripts (Niu et al., 2005). Deletion of SRF in the adult heart using a heart-specific tamoxifen-inducible Cre recombinase demonstrates its requirement for adult cardiac function and integrity. Following tamoxifen treatment, cardiac defects developed gradually from impairment of left ventricular function to dilated cardiomyopathy and eventually heart failure, with disruption of cardiomyocyte cytoarchitecture and disorganization of intercalated discs (Parlakian et al., 2005). SRF has also been shown to be required for skeletal muscle development. Specific deletion of SRF in skeletal muscle causes severe skeletal muscle hypoplasia and perinatal lethality (Li et al., 2005). These studies demonstrate the multifunctionality of SRF and its requirement for growth, differentiation, and function in striated muscle.

Concluding Remarks

Despite great pharmacological advances to enhance cardiac function, heart disease remains a major cause of morbidity and mortality (Go et al., 2013). Thus, further studies are needed to define disease mechanisms and therapeutic targets for heart disease. Altered energetics is believed to play an important role in cardiac dysfunction during heart failure, as well as modified calcium handling in response to cardiac stress. In this dissertation, transcriptional control of cardiac muscle metabolism, energy homeostasis and responsiveness of the heart to stress as modulated by the Mediator complex will be examined.

CHAPTER II

THE MEDIATOR COMPLEX: A MASTER TRANSCRIPTIONAL COORDINATOR

Introduction

Regulation of gene expression is an extremely complex process that it controlled by several different mechanisms and at multiple stages (Liu et al., 2013). Numerous signaling pathways responsible for tissue homeostasis, growth, differentiation and metabolism converge on the Mediator complex, or Mediator, through transcriptional activators and repressors that target one or more of the subunits of this complex (Malik and Roeder, 2010). The precise transcriptional activation and repression of specific genes in response to both external and internal signals is necessary for proper cell maintenance, function, and viability. Thus, more attention has recently been given to the evolutionarily conserved Mediator complex, as a general conduit and integrator of regulatory signals that converge on the promoters of protein-coding genes.

Genetic mutations of several Mediator subunits result in various human diseases, including cancers and severe developmental and neurological disorders. Kinase module subunits CDK8, cyclin C, and MED12, among a number of other core Mediator subunits have all been implicated in various forms of cancer (Firestein et al., 2008; Huang et al., 2012; Xu and Ji, 2011). Altered expression levels of MED13 and MED12 have both been

associated with human neurodevelopmental and cognitive diseases (Boutry-Kryza et al., 2012; Graham and Schwartz, 2013; Risheg et al., 2007). Here we examine the Mediator as a master transcriptional regulator and the previous studies that have implicated its specific functions within striated muscle.

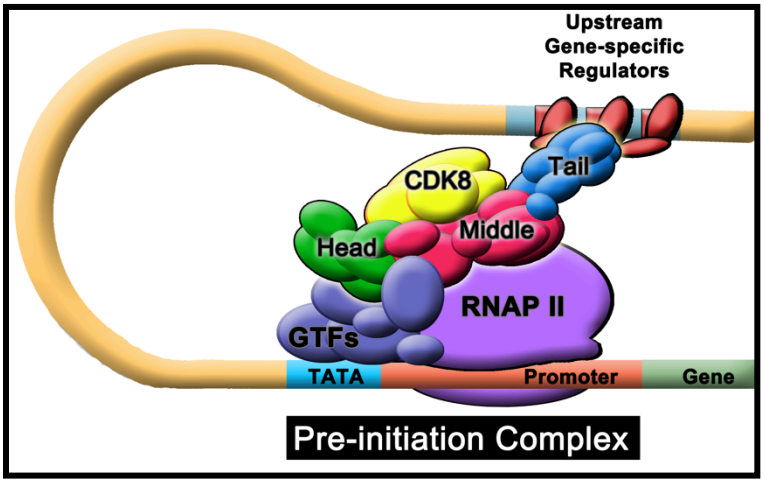

Figure 2.1 The Mediator Complex

Mediator Overview

Mediator is highly conserved from yeast through humans, and is responsible for virtually all RNA polymerase II (Pol II)-governed transcription. The multisubunit complex governs transcription by providing a bridge between upstream regulatory elements and the transcription machinery at the genetic promoter regions, stabilizing the pre-initiation complex and allowing for efficient transcription (Casamassimi and Napoli, 2007; Liu et al., 2013; Malik and Roeder, 2010). Mammalian Mediator is composed of up to 30 subunits, arranged into four distinct submodules referred to as the head, middle, tail, and kinase modules (Figure 2.1). The head, middle, and tail modules together are termed

the core complex. The kinase module, also called the CDK module, is unique to the other modules of the complex in that it has been shown to associate reversibly and transiently with the core, modulating the activity of the complex and providing either transcriptional activation or repression of certain genes. This kinase module comprises cyclin C, MED13, MED12, and cyclin-dependent kinase 8 (CDK8). In addition to the differentially associating states of the kinase module, the discovery of paralogs such as MED12-like (MED12L) has suggested that Mediator complexes containing different subunits may regulate different subsets of genes (Napoli et al., 2012). Furthermore, some subunits, such as MED26 and MED1, are not always found in all isolated Mediator complexes. Thus, current literature suggests that a minimal module may serve as a core enabling the cell to custom-design different Mediator complexes, which can then be designed in response to signals from transcription factors by the continuously changing cellular environment (Napoli et al., 2012).

Gene knockout technology and its use in creating subunit loss-of-function knockout (*null)* mice is a powerful tool for evaluating the importance of particular genes during development. Following the discovery of the Mediator complex, *null* mice for several individual Mediator subunits have been generated. Incidentally, all of these *null* mice are embryonic lethal, either early or late, with myriad different defects, suggesting a general requirement for Mediator subunits in many aspects of embryonic development (Yin and Wang, 2014).

Mediator in Striated Muscle

Currently, many studies report that different Mediator subunits are associated with specific human diseases, depending on tissue and environmental conditions (Spaeth et al., 2011). For instance, we recently found that cardiac over-expression of MED13 increases energy consumption in mice (Baskin et al., 2014; Grueter et al., 2012). These studies are ongoing and are discussed in more detail in Chapter 3. Alternatively, a mutation in MED30 was found to cause progressive cardiomyopathy and postnatal lethality (Krebs et al., 2011). These drastically different phenotypes associated with Mediator subunit manipulation suggest diverse roles for different Mediator components within the same tissue. However, the amount of studies examining the roles of Mediator subunits in the context of striated muscle is staggeringly few. Here, we will explore some of the findings that examine specific Mediator subunits in both cardiac and striated muscle.

Med30 in cardiomyopathy

Within model organisms, the Mediator complex has also been implicated in maintaining proper heart development and function and cardiomyocyte and skeletal muscle metabolism (Krebs et al., 2011; Riehle and Abel, 2012). Hypomorphic mutation of the Med30 gene, a component of the core Mediator complex, in mice leads to progressive dilated cardiomyopathy, attributed to a dramatic decline in mitochondrial oxidative phosphorylation (OXPHOS) capacity and fatty acid metabolism. These hypomorph mutant mice showed precipitous lethality 2-3 weeks post-weaning, and a

ketogenic diet attenuated this affect, extending the viability of the mice to 8.5 weeks. A ketogenic diet was found to increase cardiac expression of Ppargc1a, Esrra, Sod2, and several OXPHOS genes compared to controls (Krebs). These findings established a link between Med30 and the induction of mitochondrial metabolic pathways, with a specific impact on cardiac function.

Med1 in skeletal muscle

MED1, a component of the core Mediator complex, has been demonstrated to bind to nuclear receptors, and its deletion in skeletal muscle using muscle creatine kinase (MCK)-driven Cre recombinase enhances metabolism (Chen et al., 2010; Jia et al., 2014). MED1-deficient (Med1-mKO) mice do not show apparent morphological abnormalities, with normal growth, body fat content, glucose levels, and insulin levels in both fed and fasted states. However, glucose tolerance tests (GTT) and insulin tolerance tests (ITT) revealed enhanced glucose tolerance and insulin sensitivity in Med1-mKO mice. Moreover, when challenged with a high-fat diet, Med1-mKO mice demonstrate resistance to diet-induced obesity. Med1-mKO mice also displayed a fiber-type switch toward slower, more oxidative fibers. Accordingly, the faster muscle types also had an increased number and density of mitochondria within the tissue (Chen et al., 2010).

Microarray pathway analysis showed that a large percentage of the genes significantly up-regulated in Med1-mKO skeletal muscle tissue are involved in metabolic pathways. Notably, UCP-1 and Cidea, two mitochondrial proteins specific to brown adipose tissue were among the genes that were up-regulated most significantly, as well as

other genes known to have active roles in metabolism. The results of these studies strongly suggest that MED1 acts in skeletal muscle to regulate glucose and energy metabolism (Chen et al., 2010).

Med13 and Med12 in Drosophila muscle

Using the *Drosophila* model to examine the generality and mechanistic basis of MED13 function in muscle, it was shown that muscle–specific RNAi-mediated knockdown of the Drosophila ortholog of Med13, called *skuld (skd)*, increased adipose mass and triglyceride accumulation in adult flies (Lee et al., 2014). By utilizing the Gal4/UAS system, *skd* mRNA was targeted in somatic, cardiac, and visceral muscle tissues. Consistently, significantly increased abdominal fat bodies and total triglyceride amounts were observed in adult flies by 3 weeks of age. These studies reveal that MED13 in *Drosophila* muscle functions to suppress obesity based on several criteria, such as histology, measurement of whole-body triglycerides, tolerance to starvation

In further investigation of the mechanism behind this observed phenotype, a genetic screen was performed to identify muscle-secreted factors that regulated obesity in *Drosophila.* Among the findings was Wingless (*Wg*), the *Drosophila* ortholog of mammalian Wnt. Not only was it demonstrated in these studies that Wingless signaling in muscle is required and sufficient to suppress obesity in flies, but also that a *Wg* is epistatic to *skd*, suggesting that *Wg* is a downstream effector of MED13 in muscle. Together, these results reveal a role of muscle in systemic regulation of obesity via the function of MED13 in *Drosophila*. Interestingly, this same obesity phenotype was

observed in *Drosophila* when the Med12 ortholog, *kohtalo* (*kto*), was knocked down with the same system, suggesting that in flies, Med13 and Med12 may have similar functions in relation to systemic metabolic regulation (Lee et al., 2014).

Additional Mediator subunits

Several other Mediator subunits have demonstrated possible functions in cardiac and skeletal muscle development and function. Med13-like (MED13L) is thought to be similar enough to MED13 that some Mediator complexes may contain MED13L instead of MED13 (Muncke et al., 2003). Patient studies have revealed that mutations in the Med13L gene were linked to congenital heart defects, particularly transposition of the great arteries (TGA). Additionally, copy number changes in Med13L have recently been described in patients displaying phenotypic hypotonia and cono-truncal heart defects (Asadollahi et al., 2013).

In addition to MED1, previously mentioned as a regulator of energy homeostasis in skeletal muscle, a number of other Mediator subunits have been shown to act on metabolic signaling pathways in other tissues. These Mediator subunits could potentially have completely different activity in the context of striated muscle, and may be important keys to distinct transcriptional pathways in development and function, and warrant further study in these tissues.

Concluding Remarks

To date, many studies have indicated not only a role for Mediator in transcription initiation, but also transcriptional elongation (Conaway and Conaway, 2013) and termination (Mukundan and Ansari, 2011), mRNA processing (Huang et al., 2012), and even chromatin remodeling (Kagey et al., 2010; Zhu et al., 2011).

Genetic evidence demonstrates the importance of the components of Mediator for proper development of multi-tissue organisms. Mediator complex has been shown to play a critical role in numerous aspects of development and diseased states. The recent increase in human genetic disorders revealed to be associated with mutations in various components of the Mediator complex demonstrates the need for the development of animal models to further our understanding of this evolutionarily conserved transcription regulatory complex. Despite the vast amount of studies done deciphering the role of the Mediator complex, few studies have demonstrated tissue-specific functions for transcriptional regulation in mammals. Further investigation of the many components of Mediator in a context-specific manner is necessary. From new information, the identification and characterization of novel therapeutic targets regulating components of the Mediator complex, compounds regulating CDK8 activity, or chromatin modifying enzymes recruited by Mediator, promise to offer insight into the intricate process of Mediator-dependent transcriptional regulation in normal cardiac and skeletal muscle development and disease.

CHAPTER III

CARDIAC MEDIATOR SUBUNIT MED13 SIGNALING GOVERNS SYSTEM METABOLISM

Abstract

Obesity, type 2 diabetes, and heart failure are associated with aberrant cardiac metabolism. We show that the heart regulates systemic energy homeostasis via MED13, a subunit of the Mediator complex, which controls transcription by thyroid hormone and other nuclear hormone receptors. MED13, in turn, is negatively regulated by a heart-specific microRNA, miR-208a. Pharmacologic inhibition of miR-208a, as well as cardiac-specific overexpression of MED13, in mice confers resistance to high-fat diet-induced obesity and improves systemic insulin sensitivity and glucose tolerance. Conversely, genetic deletion of MED13 specifically in cardiomyocytes enhances obesity in response to high-fat diet and exacerbates metabolic syndrome. The metabolic actions of MED13 result from increased energy expenditure and regulation of numerous genes involved in energy balance in the heart. These findings reveal a role of the heart in systemic metabolic control and point to MED13 as a potential therapeutic target for metabolic disorders.

Introduction

Through earlier genetic knockout work, it was found that the miR-208a, a cardiac muscle-specific mircoRNA (miRNA or myomiR) encoded by an intron of the αMHC gene, is required for cardiac fibrosis and expression of βMHC in response to stress and hypothyroidism. In the absence of miR-208, the expression level of βMHC is severely blunted in the adult heart in response to activated calcineurin, pressure overload, or hypothyroidism, suggesting that the pathways through which these stimuli induce βMHC transcription share a common miR-208–sensitive component (van Rooij et al., 2007). Through pharmacological inhibition of miR-208a by specific locked nucleic acid (LNA)-antisense oligonucleotides, cardiac function was shown to be enhanced in a rat model of diastolic dysfunction (Montgomery et al., 2011). Additionally, miR-208a was demonstrated to regulate T3-dependent repression of βMHC, through targeting the mRNA transcript of Med13 for repression. MED13, also called Thyroid hormone receptor Associated Protein 1 (THRAP1), was previously shown to be a coregulator of thyroid hormone receptor (TR) signaling (Pavri et al., 2005).

Further investigation of miR-208a revealed that LNA antimiR-208a-treated mice displayed resistance to high-fat diet-induced glucose intolerance compared to controls. In contrast to the control groups, the antimiR-208a-treated mice on high-fat diet did not gain as much fat mass, lower fasting insulin levels, lower leptin levels, and displayed improved whole-body insulin sensitivity (Grueter et al., 2012). Together, these results suggest that miR-208a acts on systemic metabolism by repressing expression of the TR coregulator MED13/THRAP1. Moreover, hearts of mice lacking miR-208 are insensitive

to stress and hypothyroidism, pointing to miR-208 and MED13 as important regulators of heart disease and TH sensitivity (van Rooij et al., 2007). With the ubiquitous protein MED13 brought to our attention, we used gain- and loss-of function genetics in mice to identify the role of cardiac MED13 in a tissue-specific manner, uncovering its function in cardiac metabolism and systemic energy regulation.

Results

Cardiac-Specific Overexpression of Med13 Prevents Obesity and Improves Glucose Tolerance

To determine if elevation of MED13 in the heart might evoke metabolic effects analogous to those we observed with miR-208a inhibition, we generated transgenic mice overexpressing MED13 driven by the cardiomyocyte-specifc αMHC (alpha-myosin heavy chain) promoter. We generated two independent αMHC-Med13 transgenic (TG) mouse lines, referred to as Lines 1 and 2, showing 9- and 3-fold increases, respectively, in expression of Med13 mRNA and protein compared to wild-type (WT) in the heart (Figure 3.1A and 3.1B). Neither αMHC-Med13 TG mouse line showed overt abnormalities, and gross cardiac structure was normal with non-significant elevation in cardiac stress markers (Figure 3.1C and 3.1D).

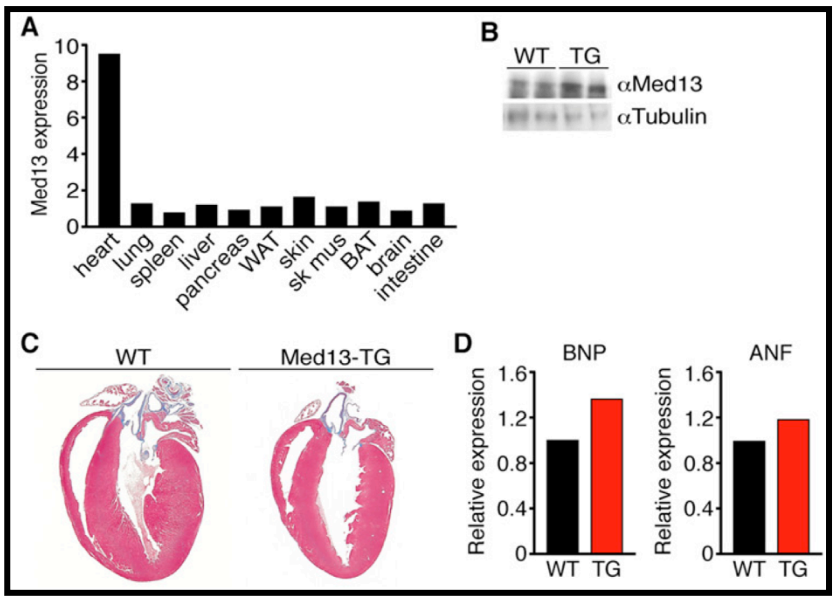

Figure 3.1. Med13 Overexpression in Heart Tissue.
(A) Multitissue analysis comparing Med13 mRNA levels from aMHC-Med13 TG mice compared to WT mice by quantitative RT-PCR.
(B) Representative immunoblot of Med13 from WT and aMHC-Med13 TG hearts. Anti-tubulin was used as loading control.
(C) H&E stain of aMHC-Med13 TG and WT mouse hearts.
(D) BNP and ANF mRNA levels in aMHC-Med13 TG and WT mice on normal chow (NC).

Male αMHC-Med13 TG mice were comparable in length to WT littermates, although they were lighter when fed normal chow (NC), and were more resistant to obesity on high-fat (HF) diet (Figures 3.2A–C). Compared to WT littermates, adult αMHC-Med13 TG mice had significantly less fat mass on both the NC and HF diet as measured by NMR (Figure 3.2D). Interscapular brown adipose tissue (BAT) and visceral WAT mass from the αMHC-Med13 TG mice on HF diet and NC were reduced compared to WT mice at the same conditions (Figure 3.2E). Gross and histological analysis of interscapular fat from αMHC-Med13 TG mice showed less lipid accumulation on NC and HF diet compared to WT mice, as well as decreased adipocyte size of WAT (Figures

3.2F and 3.2G). Similarly, αMHC-Med13 TG mice at 7 and 12 months of age also had significantly less fat mass than WT littermates while on normal chow (Figure 3.2H).

Given the dramatic changes in adipose tissue mass, we next analyzed several metabolic tissues for lipid accumulation through Oil-Red O staining. Cardiac tissue from WT and αMHC-Med13 TG mice on NC or HF diet displayed no differences in lipid accumulation or triglyceride levels (Figure 3.2I and 3.2J). However, WT mice on HF diet demonstrated highly elevated hepatic lipid and triglyceride accumulation, but levels in αMHC-Med13 TG mice were not significantly different from WT mice on NC (Figure 3.2I and 3.2K). Serum triglyceride and cholesterol levels were also diminished in αMHC-Med13 TG mice compared to WT on HF diet (Figure 3.2L and 3.2M). In addition, αMHC-Med13 TG mice showed a normal glucose response after 6 weeks of HF diet compared to the glucose intolerance seen in WT mice (Figure 3.2N). Together this data suggests that whole-body insulin sensitivity following HF diet is improved with cardiac overexpression of Med13.

Cardiac deletion of Med13 enhances susceptibility to obesity

In further investigation of the role of cardiac-specific Med13 in systemic metabolism, we generated mice with a conditional Med13 loss-of-function allele. Through the introduction of loxP sites, Cre-mediated excision of exons 7 and 8 results in a frame shift and loss of a majority of the MED13 coding sequence, including the putative NLS, NR binding motifs, leucine zipper and FoxO-like domain (Figure 3.3A). Cardiac-specific deletion of MED13 was accomplished through breeding floxed mice

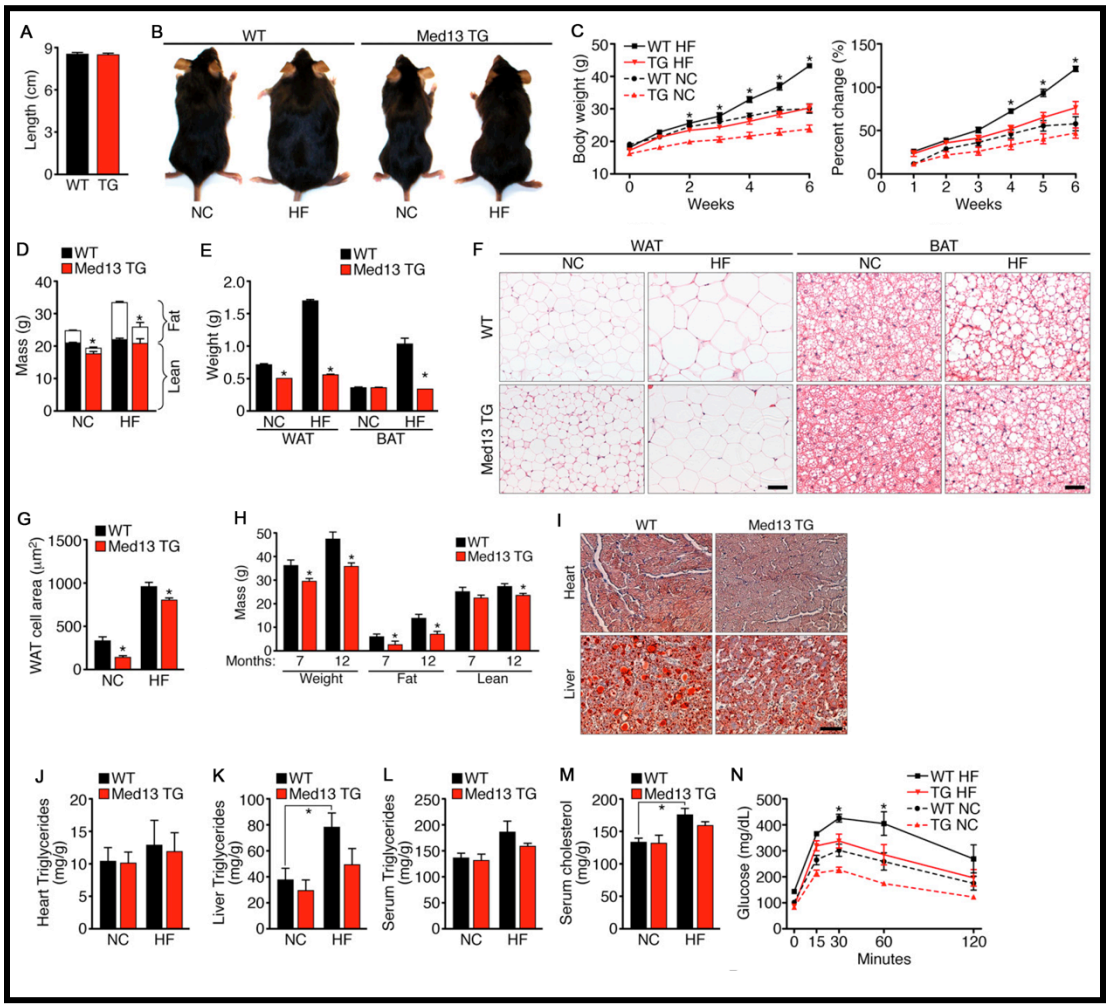

Figure 3.2. Cardiac-Specific Overexpression of Med13 Prevents Obesity and Improves Glucose Tolerance

(A) Nose-to-anus length for 12 week old aMHC-Med13 TG and WT mice on NC.
(B) Pictures of male WT and aMHC-Med13 TG mice after 6 weeks on NC or HF diet.
(C) Growth curves and percentage increase in body weight.
(D) Body composition as measured by NMR to determine fat and lean tissue mass.
(E) Weight of visceral WAT and interscapular BAT.
(F) H&E stain of visceral WAT and subscapular BAT. Scale bar, 40 mm.
(G) Cell size of visceral WAT. Values represent the mean cross-section area of each cell. Images from three sections 200 mm apart were analyzed from seven to eight mice in each group, representing > 500 cells.
(H) Body composition analysis of aMHC-Med13 TG compared to WT mice at 7 and 12 months of age on NC. N = 3-5.
(I) Oil red O stained hearts and liver from HF diet treated aMHC-Med13 TG and WT mice. Scale bar, 40 mm.
(J–L) Heart, liver, and serum triglyceride levels.
(M) Serum cholesterol levels.
(N) Glucose tolerance test (GTT).
Data are represented as mean ± SEM. *P < 0.05 aMHC-Med13 TG versus WT.

with mice expressing Cre-recombinase in cardiomyocytes under the control of the αMHC promoter. Analysis of Med13 expression in Med13fl/fl;αMHC-Cre mice by qPCR revealed a reduction of Med13 transcript levels in whole heart by 60% (Figure 3.3C). Cardiac knockout (cKO) mice were born at Mendelian ratios and demonstrated no overt changes in cardiac function or morphology (Figure 3.3B-G).

To assess the potential metabolic consequences of cardiac MED13 deletion, we placed adult 6 week-old Med13 cKO mice on HF diet. Initially, the Med13 cKO mice weighed the same as their WT littermates, but gained significantly more weight beginning within the first week on HF diet and continuing throughout the study (Figure 3.4A and 3.4B). After 6 weeks on HF diet, we observed a dramatic increase in fat mass in the Med13 cKO mice compared to Med13fl/fl control littermates on HF diet (Figure 3.4C and 3.4E). Heart weight/ body weight ratios were not significantly different in Med13 cKO mice compared to Med13fl/fl controls (Figure 3.4D).

Med13 cKO mice had significantly larger visceral white adipose, interscapular brown fat and liver mass than controls on HF diet (Figure 3.4Q). Histological analysis of these tissues revealed an increase in lipid accumulation in the Med13 cKO versus Med13fl/fl mice (Figure 3.4F and 3.4I). Liver triglycerides, as well as serum triglycerides, cholesterol and blood glucose levels were also elevated in the Med13 cKO animals (Figure 3.4J–N). Fasting insulin levels in the Med13 cKO mice were highly variable but were dramatically increased, as were leptin levels (Figures 3.4O and 3.4P). Thus, cardiac deletion of MED13 perturbs whole-body metabolism, enhancing sensitivity to HF diet, a phenotype opposite that of Med13 TG or antimiR-208a treated mice.

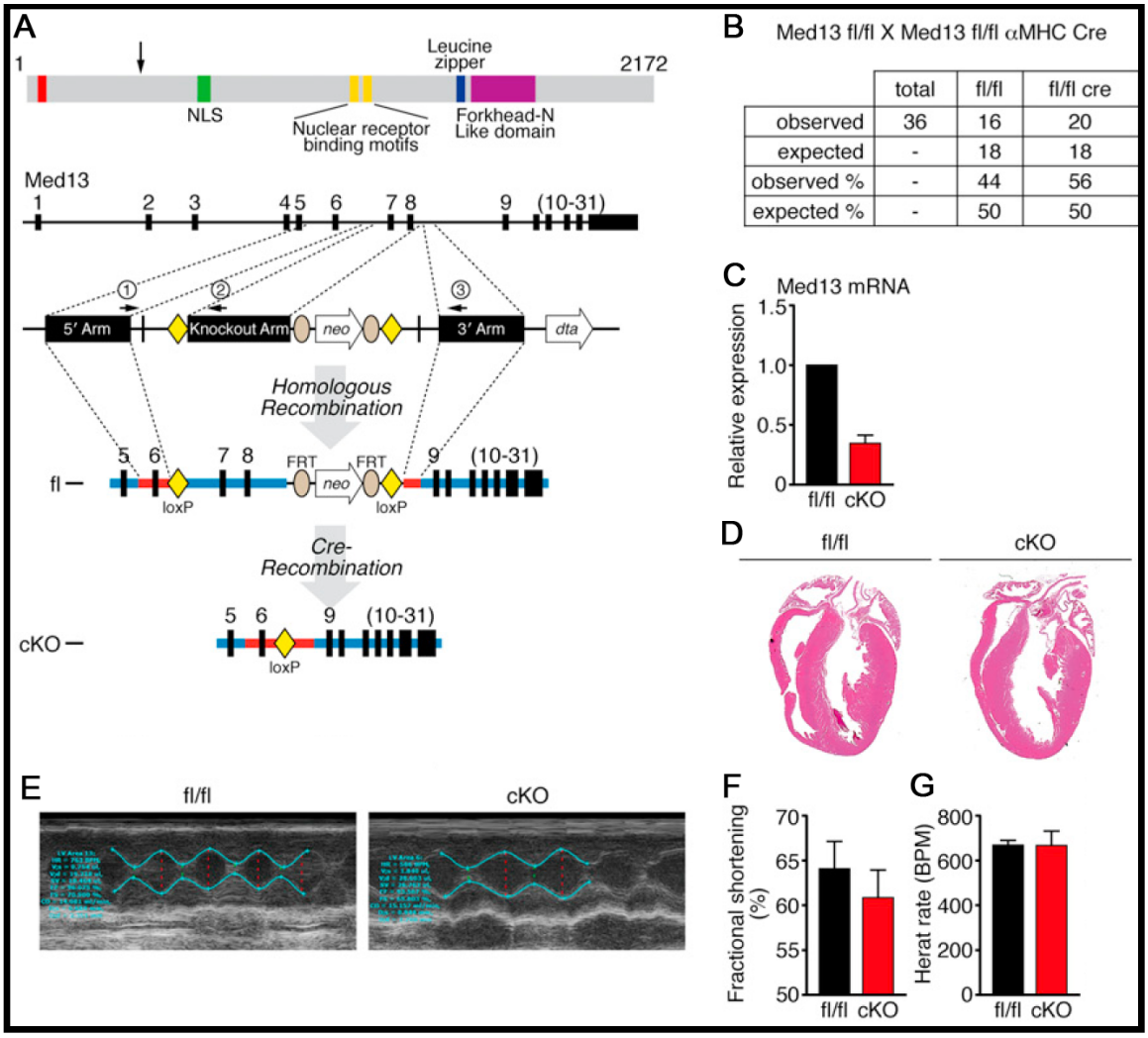

Figure 3.3. Conditional Deletion of Med13 in Cardiomyocytes
(A) Schematic diagram of putative MED13 protein domains, the arrow represents the end of the MED13 resulting from targeted gene deletion. Arms of homology flanking exons 7 and 8 were used to insert loxP sites, a neomycin cassette and DTA for homologous recombination. Cre-mediated recombination of the Med13 cKO removes exons 7 and 8.
(B) Med13-cKO conditional knockout offspring chart.
(C) Expression of Med13 mRNA in heart, N = 3.
(D) H&E stain of 6 week old Med13-cKO and Med13fl/fl hearts.
(E) Representative traces of an echocardiograph from Med13fl/fl; aMHC-Cre and Med13fl/fl.
(F) Cardiac fractional shortening from Med13-cKO and Med13fl/fl mice. N = 5-7.
(G) Heart rate from Med13-cKO and Med13fl/fl mice. N = 5-7.

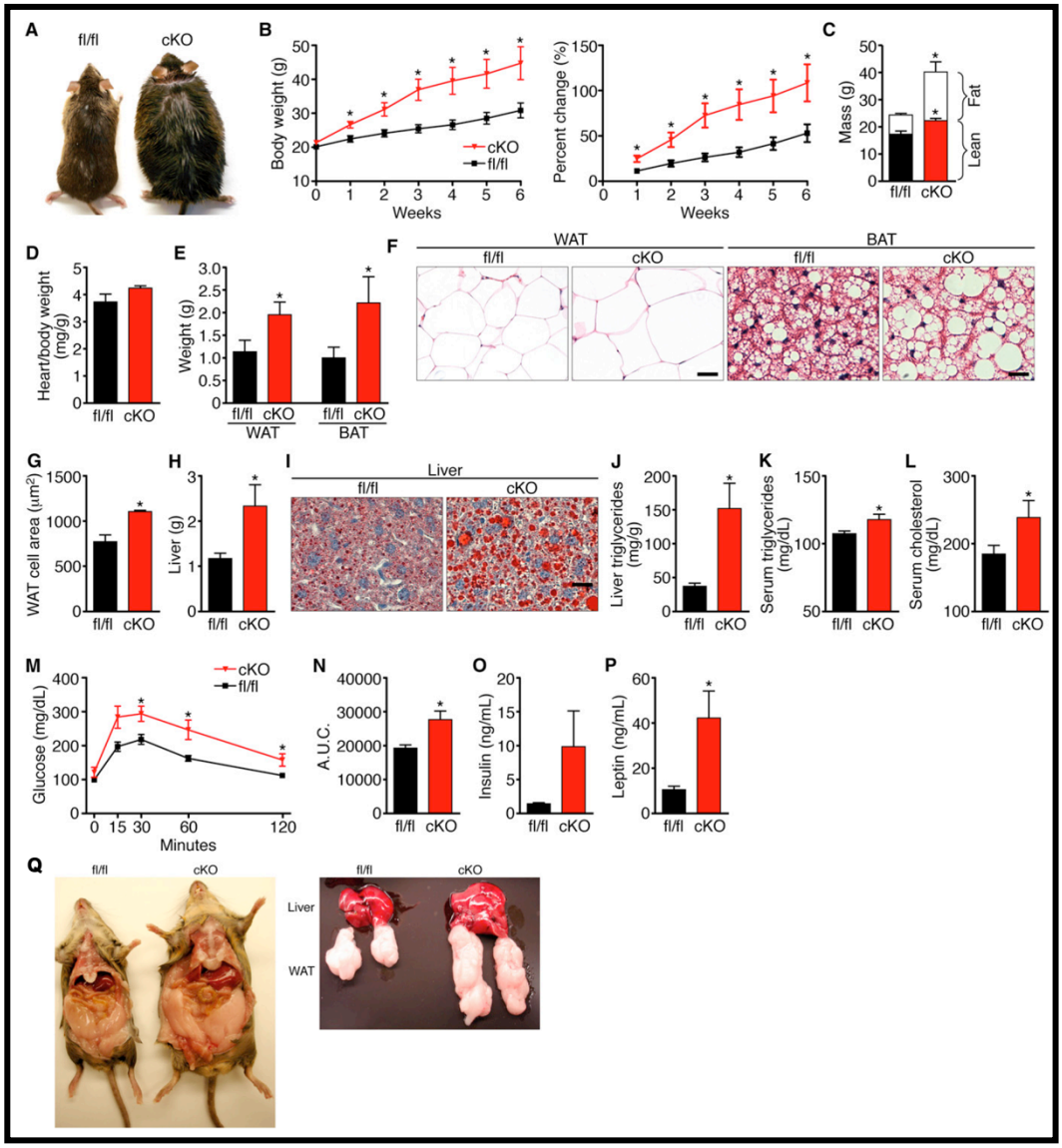

Figure 3.4. Cardiac deletion of Med13 Enhances Susceptibility to Obesity
(A) Representative images of Med13-cKO and fl/fl mice on HF diet for 6 weeks.
(B) Growth curves and percentage increase in body weight.
(C) Body composition measured by NMR to determine fat mass and lean tissue mass of Med13-cKO and fl/fl mice following 6 weeks on HF.
(D) Heart weight/body weight ratio.
(E) Weight of visceral WAT and subscapular fat.
(F) H&E stained visceral WAT and BAT. Scale bar, 40 mm.
(G) Cell size of visceral WAT. N = 5.
(H) Whole liver tissue mass.
(I) Oil-red O staining of liver sections. Scale bar, 40 mm.
(J) Liver triglyceride content. N = 6–8.
(K) Serum triglyceride content. N = 6–8.
(L) Serum cholesterol levels. N = 6–8.

(M) Glucose tolerance test (GTT). N = 6–8.
(N) Area under the curve for the GTT. N = 6–8.
(O) Fasting insulin levels. N=6.
(P) Fasting leptin levels. N = 6.
(Q) Med13fl/fl and Med13-cKO images displaying disproportionate WAT mass and discolored fatty liver in mice after 12 weeks on HF diet.
N=8-10 unless otherwise noted. Data are represented as mean ± SEM. *P < 0.05.

MED13 modulates systemic energy consumption

The resistance to weight gain by αMHC-Med13 TG mice was not due to a difference in food consumption, physical activity, core body temperature compared to WT mice, as measured using metabolic chambers (Figure 3.5A and 3.5B). Remarkably, however, lean weight-matched αMHC-Med13 TG mice exhibited an increase in oxygen consumption and carbon dioxide production, suggesting that the observed decrease in fat mass was due to an increase in systemic energy consumption mediated by over-expression of MED13 in the heart (Figure 3.5C and 3.5D).

Down-regulation of Nuclear Hormone Receptor target genes by MED13

To further explore the molecular basis of the changes in energy homeostasis caused by cardiac overexpression of MED13, we performed microarray analysis on mRNA isolated from WT and αMHC-Med13 TG hearts. Microarray profiling and gene ontology analysis revealed 96 gene transcripts regulated by more than 2-fold in αMHC-Med13 TG hearts, with 34 genes up-regulated and 62 genes down-regulated (Figure 3.6A). Real-time (RT-PCR) validated these results (Figure 3.6B). Though the up-regulated transcripts in αMHC-Med13 TG hearts did not appear to fit a specific pattern,

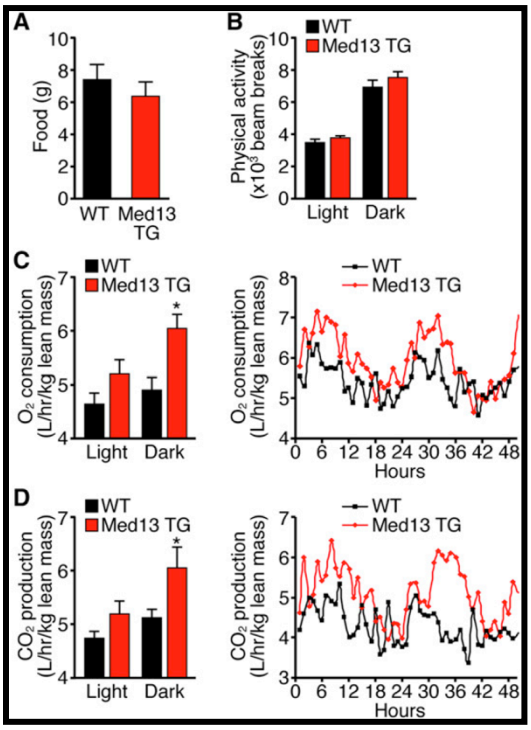

Figure 3.5. MED13 Modulates Systemic Energy Consumption
(A) Food consumption by 12-week-old male WT and Med13-cKO.
(B) Physical activity and average beam breaks in the x, y, and z axis over a 12-hr light/dark cycle.
(C) Average oxygen consumption per hour during the light/dark cycle (left); average traces (right) normalized to lean mass.
(D) Average carbon dioxide production per hour during the light/dark cycle (left); averages traces (right) normalized to lean mass.
Data are represented as mean ± SEM. *P < 0.05 versus WT.

there was a significant majority of down-regulated genes were involved in metabolism and known to be regulated by NRs (Figure 3.6A and 3.6C).

Further analysis of the gene sets revealed that many of the down-regulated genes in αMHC-Med13 TG hearts are known targets of NRs (TR, RXR, LXR), consistent with the model of repressive influence of MED13 on NR activity (Figure 3.6C). Other transcription factors involved in metabolic regulation (PPARγ, NCoR and SREBP) were also identified as regulatory hubs in the control of MED13-responsive genes. Moreover,

mice with genetic deletion of several genes that were down-regulated (Thrsp, Elovl6, Gpd2, Eno1, Cidea, Tkt or PPARγ) display resistance to diet-induced obesity and/or protection against insulin resistance (Anderson et al., 2009; Jones et al., 2005; Xu et al., 2002; Zhou et al., 2003). These findings suggest that cardiac MED13 acts to inhibit expression of a set of NR-responsive genes, thereby altering whole-body energy homeostasis.

As we know that cardiac over-expression of MED13 reduces fat accumulation in peripheral tissues, we also performed microarray analysis on interscapular BAT, visceral WAT and liver tissues from 4 week-old WT and αMHC-Med13 TG mice littermates (Figure 3.6D). Gene ontology analysis of the genes regulated greater than 2-fold revealed that genes associated with metabolic processes were the most strongly affected in cardiac and non-cardiac tissues of αMHC-Med13 TG mice (Thomas et al., 2006).

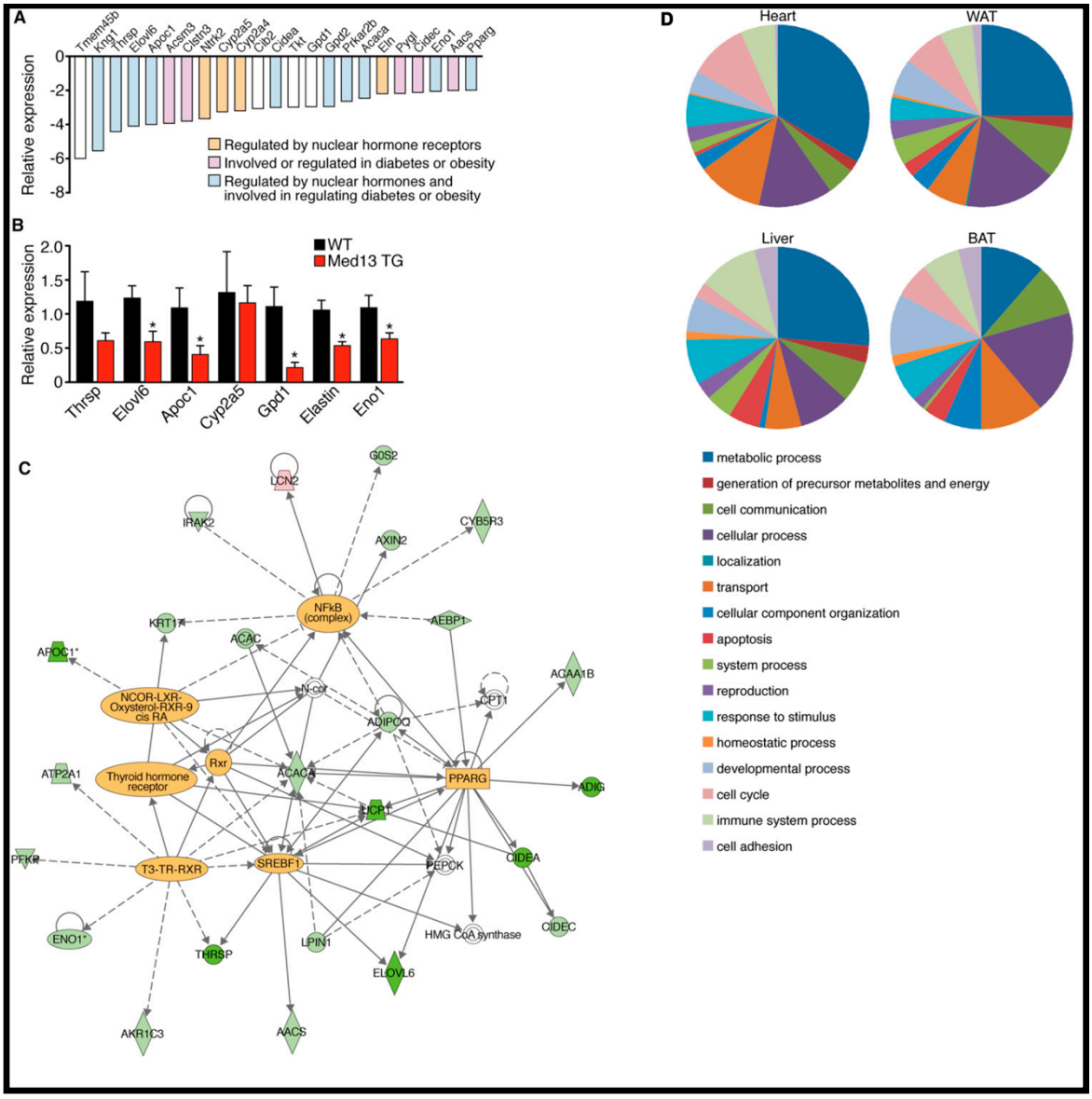

Figure 3.6. Down-regulation of Nuclear Hormone Receptor Target Genes by Med13
(A) Microarray analysis of genes down-regulated in hearts from adult aMHC-Med13 TG mice compared to WT mice.
(B) Real-time qPCR of select genes identified in (A) comparing aMHC-Med13 TG and WT mice.
(C) Ontology/Pathway analysis of genes regulated > 1.5- fold in the aMHC-Med13 TG cardiac tissue array. Highlighted in yellow within the diagram are transcription factors that function as nodal points for genes regulated in aMHC-Med13 TG mouse hearts.
(D) Analysis of Heart, WAT, BAT, and liver microarray data comparing 4-week-old aMHC-Med13 TG and WT mice. Sections of the pie chart make up the total genes dysregulated by greater than 2-fold and the ontology categorization under which they fall.
N = 4–5. Data are represented as mean ± SEM. *P < 0.05 versus WT.

Discussion

The liver, adipose tissue and skeletal muscle are well known to function as the major tissue regulators of whole-body energy expenditure, metabolism and glucose homeostasis. These findings demonstrate that the heart, known to have the highest rate of oxygen consumption per gram of any tissue in the body (Rolfe and Brown, 1997) plays an important role in the control of energy homeostasis and adiposity. The enhanced whole body energy expenditure resulting from cardiac over-expression of MED13 may result from suppression of metabolic genes in the heart and consequent compensatory metabolic activity in non-cardiac tissues. Alternatively, MED13 also may regulate systemic energy storage and consumption through a cardiac-derived paracrine factor acting on distal tissues either directly or through secondary targets such as the brain. The heart has been shown to exert endocrine effects by releasing natriuretic peptides, ANP and BNP (Sengenes et al., 2000). However, we did not observe altered expression of ANP or BNP in mice with MED13 gain- or loss-of-function. Considering that disturbance of cardiac energy metabolism is among the earliest alterations in the heart during the development of diabetes (Harmancey et al., 2008), it will be of interest to investigate the potential involvement of the MED13-miR-208a regulatory circuit in this disorder.

Control of energy homeostasis by cardiac MED13

The Mediator complex links gene-specific transcription factors with the basal transcriptional machinery (Ito and Roeder, 2001). The kinase submodule of Mediator, comprising MED12, MED13, CDK8 and cyclin C, has been shown to activate or repress expression of select target gene sets in certain instances by interfering with or stabilizing the association of Mediator and RNA Pol II (Agostini et al., 2006; Belakavadi and Fondell, 2010; Conaway and Conaway, 2011; Donner et al., 2007; Knuesel et al., 2009a). Though the importance of the Mediator complex in the control of gene transcription has been well established from in vitro transcription assays (Conaway and Conaway, 2011; Malik and Roeder, 2010), determination of the functions of this complex in adult tissues has been hindered due to early lethality observed in all mutant alleles of Mediator subunits analyzed to date. At publication of this study, no functions had been attributed to MED13 in any mammalian tissues nor had potential functions of any components of the Mediator complex been analyzed in the heart.

Through cardiac-specific gain- and loss-of-function of MED13 in mice, these results highlight a central role of this Mediator subunit in governance of metabolism through the control of energy expenditure pathways. The finding that MED13 deficiency in the heart causes dramatic obesity in mice on HF diet is consistent with a recent report that MED13 deficiency in muscle of Drosophila causes enhanced lipid accumulation in the fat body (Lee et al., 2014; Pospisilik et al., 2010) and suggests an evolutionarily conserved role for MED13 in the control of metabolic homeostasis by striated muscles of metazoans. As mentioned previously, genetic deletion of MED1 in skeletal muscle of

mice confers resistance to diet-induced obesity (Chen et al., 2010), analogous to the phenotype we observed with over-expression of MED13 in the heart. MED1, a core component of the Mediator complex, controls transcriptional activation through direct interaction with numerous NRs (Ge et al., 2002; Ito et al., 2000; Malik et al., 2004). Though MED13 has never been found to interact directly with NRs, it is thought in some conditions to function as a transcriptional repressor through steric hindrance of the association of RNA Pol II with the core Mediator complex. Therefore the actions of MED13 on NRs are consistent with the opposing influences of MED13 on MED1 (Knuesel et al., 2009a).

MED13-mediated modulation of cardiac TH and NR signaling

TH is a major determinant of metabolic rate, energy expenditure and cardiac contractility (Song et al., 2011). When MED13 is over-expressed in the cardiac tissue, the mice display increased energy expenditure and resistance to visceral adipose accumulation, a phenotype similar to that of enhanced TH signaling in mice and humans, (Watanabe et al., 2006). However, only a subset of TH-dependent genes are modulated in response to MED13 over- expression in the heart. TH stimulates and represses TR-dependent genes depending on transcriptional cofactors and intracellular signals (Fondell et al., 1999). Consistent with a repressive influence, MED13 blocked transcription of TRβ reporter genes in vitro, and transgenic over-expression of MED13 in the heart suppressed a broad collection of TR and NR target genes involved in energy balance. Among the genes down-regulated by MED13, deletion of Thrsp, Gpd2, Eno1, Aacs and

Pparg in mice results in resistance to diet-induced obesity (Anderson et al., 2009; Jones et al., 2005; Xu et al., 2002; Zhou et al., 2003), as we observed in response to cardiac over-expression of Med13. Elovl6 and Kng1, which are repressed by MED13, modulate insulin and glucose homeostasis (Matsuzaka et al., 2007; Wu et al., 2010).

In addition to regulating a subset of TR targets, gene network analysis indicates a role for MED13 in the control of other transcriptional regulators of lipid biosynthesis and metabolism, including NCoR1, SREBP, LXR, RXR and PPARγ. It is notable in this regard that inhibition of SREBP, RXR, and PPARγ ameliorates diet-induced obesity and type 2 diabetes (Finck et al., 2002; Jones et al., 2005; Yang et al., 2006). Conversely, cardiac- specific over-expression of PPARα causes metabolic cardiomyopathy and hepatic insulin resistance (Finck et al., 2002). Thus, MED13 appears to function in the heart as a master regulator of the transcriptional circuitry responsible for metabolic homeostasis by suppressing the actions of multiple metabolic regulators.

Therapeutic implications of miR-208a and Med13 studies

TH signaling confers numerous beneficial effects, including increased metabolic rate, lipolysis, cholesterol lowering, improved glucose homeostasis, and enhanced cardiac function as seen in antimiR-208a treated and αMHC-Med13 TG mice (Crunkhorn and Patti, 2008; Song et al., 2011; Watanabe et al., 2006). However, hyperthyroidism is also associated with adverse effects, such as tachycardia, arrhythmias, muscle wasting and elevated body temperature, which we did not observe in these mice. There have been numerous efforts to develop TH mimetics for enhancing cardiac function and improving

metabolic status, but the adverse side-effects of TH stimulation have limited the usefulness of such compounds (Tancevski et al., 2011). AntimiR-208a seems to display the beneficial activities of thyromimetics, however, the target of antimiR-208a is cardiac-specific, thereby bypassing potential adverse effects on other tissues where TH exerts its effects. The apparent metabolic effects of miR-208a inhibition and MED13 elevation in the heart suggest that miR-208a inhibitors, in addition to providing benefit in the setting of cardiac dysfunction, may have therapeutic usefulness in a variety of metabolic disorders, such as obesity, hypercholesterolemia, type 2 diabetes, hepatic steatosis and hyperlipidemia.

Following our MED13 studies, we saw that, intriguingly, humans with mutations in MED12 exhibit hypothyroidism and are predisposed to obesity (Philibert et al., 2002). This suggests that MED12 exerts metabolic functions in certain contexts, and led us to further analyze the role of MED12 in striated muscle tissues. These studies will be further discussed in the next two chapters.

Methods

Generation of αMHC-Med13 TG mice. Med13 was overexpressed specifically in cardiac tissues as previously described (Subramaniam et al., 1991). In brief, Med13 cDNA was cloned into a plasmid containing the αMHC promoter and human GH (hGH) poly(A)+ signal.

Generation of αMHC-Cre-Med13 cKO mice. Arms of homology flanking exons 7 and 8 were used to insert loxP sites, a neomycin cassette and DTA for homologous recombination. Cre-mediated excision was performed through breeding female animals homozygous for floxed Med13 alleles, with male transgenic mice expressing one allele of Cre recombinase driven by the αMHC promoter.

Glucose tolerance tests. Glucose tolerance tests were performed following overnight fasting. Baseline measurements were taken using an Accu-Chek Compact Plus glucometer (Roche). Mice were subsequently injected with 1mg/g glucose intraperitoneally. Glucose levels were then measured at 15, 30, 60 and 120 minutes following glucose injection.

NMR. Male mice body composition parameters including fat mass, lean tissue mass and water were analyzed using a Bruker Minispec mq10.

Transthoracic echocardiography. Cardiac function was evaluated by two-dimensional transthoracic echocardiography on conscious adult mice (8-16 wks). The largest anteroposterior diameters in diastole and systole were assessed in at least three recorded M-mode tracings and LV fractional shortening calculated according to the formula FS(%) = [(LVIDd – LVIDs)/LVIDd] × 100. All measurements were performed by a single experienced operator blinded to the mouse genotypes.

RNA Analysis. RNA was isolated from mouse tissues using TRIzol reagent (Invitrogen). RT-PCR was performed to generate cDNA. For qPCR, 20 ng of cDNA was used for each reaction with Taqman or SYBRgreen probes and normalized to 18S expression.

Microarray analysis. Microarray analysis was performed by the University of Texas Southwestern Microarray Core Facility using the MouseWG-6 v2.0 BeadChips (Illumina) using RNA extracted from 4-week old WT or αMHC-Med13 TG mice (N=3) and subsequently pooled prior to analysis.

Animal Care. Animals were fed standard chow with 4% kcal from fat ad lib unless otherwise noted. HF diet analyses were done using a 60% kcal from fat diet or a 10% kcal from fat as the NC-control diet (Open Source Diets D12492i and D12450Bi). Propylthiouracil (PTU) treatment was administered in the chow at 0.15% for 2 weeks (Harlan Teklad). All animal procedures were approved by the Institutional Animal Care and Use Committee at UT Southwestern Medical Center.

CHAPTER IV

CARDIAC MED12 REGULATES EXPRESSION OF GENES INVOLVED IN CONTRACTILITY

Introduction

In light of the dramatic effect of cardiac overexpression or deletion of MED13 on global metabolism, we decided to explore the potential functions of the ubiquitous Mediator subunits in heart metabolism and function. As stated previously, MED13 resides in the kinase module of Mediator, along with cyclin C, CDK8, and MED12, which has been previously found in some studies to regulate the kinase activity of CDK8 (Knuesel et al., 2009a; Knuesel et al., 2009b). MED12 is an accessory subunit to Mediator that has had ties to such diseases as cancer (most commonly uterine leiomyomas) and Optiz-Keveggia syndrome, but the specific function of this subunit in various tissues has not been explored.

In invertebrates, MED12 and MED13 were shown to act redundantly in some developmental processes (Janody et al., 2003; Lee et al., 2014; Steimel et al., 2013; Treisman, 2001). In zebrafish, MED12 is required for development of the neural crest, endoderm, kidney, brain, and heart (Hong et al., 2005; Rau et al., 2006; Shin et al., 2008; Wang et al., 2006).

The first study of MED12 function in mice was not published until very recently in 2010 (Rocha et al., 2010b). Ablation of MED12 leads to embryonic lethality by E7.5

due to failure of mesoderm formation and abrogated Wnt/β-catenin signaling. Thus, the researchers created a mouse line that expressed a very low level of Med12 mRNA, referred to as Med12 hypomorphs, in order to study the effect on the embryos at a later developmental stage. The Med12 hypomorph embryos demonstrated developmental arrest at E10.5 during embryogenesis with defects in neural tube closure, axis elongation, somitogenesis and heart development (Rocha et al., 2010b). Through these studies, Med12 was found to be an essential coregulator of transcription factors controlling gene-specific functions during mouse development, including correct Wnt/β-catenin signaling and planar cell polarity.

Mutations in MED12 have been described in human patients, as well, often in association with X-linked intellectual disability syndromes (Graham and Schwartz, 2013). In 2007, Risheg et al., reported on the first instance of intellectual disability syndrome linked with a recurrent missense mutation in Med12 on the X chromosome (Risheg et al., 2007). This disorder was described as Opitz-Kaveggia syndrome, also known as FG syndrome-1. Later that same year, another missense mutation in Med12 was reported in a family with Lujan syndrome (Schwartz et al., 2007), and more recently another novel Med12 missense mutation was linked to Ohdo syndrome (Graham and Schwartz, 2013). Other symptoms that overlap between the syndromes include craniofacial defects, constipation, hypotonia, and congenital heart defects (Clark et al., 2009). This links Med12 to heart defects in humans as well as zebrafish and embryonic mice.

Here we show that deletion of MED12 specifically within cardiac muscle leads to dysregulation of several genes involved in calcium signaling and muscle function. These findings unveil a previously unrecognized role for MED12 in heart contractility.

Results

Cardiac-specific deletion of MED12 leads to dilated cardiomyopathy

Global deletion of Med12 in mice results in embryonic lethality by E7.5 due to an inability to form mesoderm and abrogated Wnt/β-catenin signaling (Rocha et al., 2010b). Comparison of ventricular mRNA levels by qPCR at different stages of embryonic and postnatal development revealed that Med12 expression does not differ significantly during development (Figure 4.1A). To determine the functional role of MED12 in the heart, we bred mice conditionally targeted at the Med12 locus (Rocha et al., 2010a) with mice expressing Cre-recombinase driven by the cardiomyocyte-specific αMHC promoter (Agah et al., 1997). Male Med12fl/Y; αMHC-Cre conditional (cardiac) knockout mice (referred to as Med12-cKO mice) were born at Mendelian ratios and appeared identical to Med12 fl/Y littermate controls (CTL) which lacked the Cre allele. Analysis of Med12 mRNA expression in 10-week old Med12-cKO mice by qPCR revealed a 60% reduction in Med12 transcript levels in cardiac tissue (Figure 4.1B). Residual cardiac expression is likely to reflect the presence of non-myocytes that comprise up to half of the cells of the heart.

Hearts of CTL and Med12-cKO mice were indistinguishable morphologically at birth but gradually displayed ventricular wall thinning and dilation beginning by postnatal day P7. Post-weaning, Med12-cKO mouse hearts already weighed significantly more than CTL hearts, and by 12 weeks of age, hearts from Md12-cKO mice weighed on average 60% more than those of CTL when normalized to tibia length (Figure 4.1C). Histological staining of frontal sections revealed that by postnatal stage P7 the Med12-cKO mice exhibited chamber dilation was evident in both ventricles, with the severity of dilation increasing with age to ultimately affect both ventricles and right atrium (Figure 4.1D).

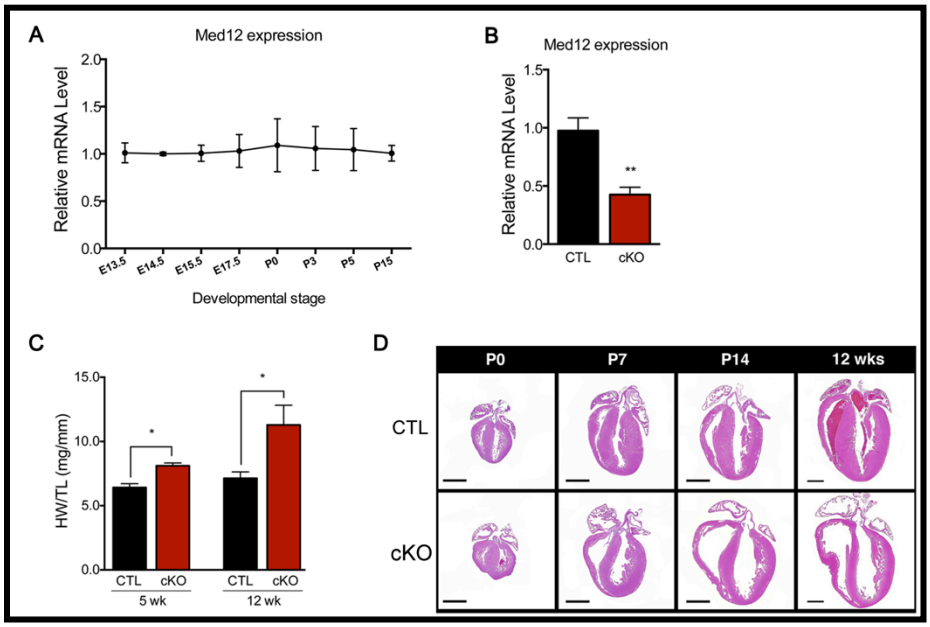

Figure 4.1. Med12 deletion in Cardiomyocytes Leads to Dilated Cardiomyopathy.
(A) Med12 mRNA transcript levels at various points of embryonic and postnatal development.
(B) Relative Med12 mRNA expression levels in whole heart tissue measured by qPCR.
(C) Average heart weights from 5-week and 12-week-old mice, normalized to tibia lengths.
(D) Representative H&E stains of frontal sections of hearts from CTL (top) and MED12 cardiac knockout (bottom) mice from various stages of postnatal development. Scale bar, 1mm.
N=5-8 per group. Data are represented as ± SEM. *P < 0.05, **P < 0.01.

To confirm the extent of impaired cardiac function in vivo, mutant mice were analyzed by trans-thoracic echocardiography. Med12-cKO mice at 6 weeks of age showed dilated hearts with poor contractility (Figure 4.2A). Moreover, echocardiography indicated impaired heart rate and cardiac contractility as early as P3, which progressively continued to decline with age (Figure 4.2B), consistent with the histological phenotype of dilated cardiomyopathy.

Further histopathological investigation of Masson's trichrome-stained sections from adult Med12-cKO hearts revealed diffuse interstitial fibrosis, indicative of heart failure (Figure 4.2C). Electron microscopy of longitudinal sections of ventricles from CTL and Med12-cKO mice at 8 weeks old showed no abnormalities in sarcomeric structure in mutant hearts (Figure 4.2D).

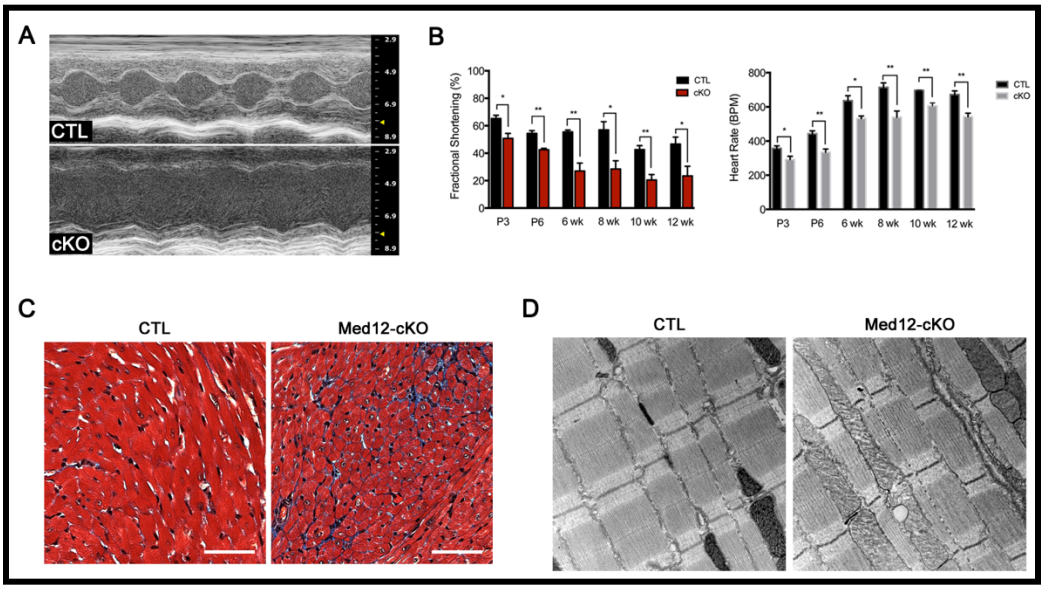

Figure 4.2 Functional Defects in Med12-cKO Hearts.
(A) Echocardiograms taken from 6 week-old male littermates.
(B) Fractional shortening and heart rate measured by echocardiography of animals from various points in postnatal development.

(C) Masson's trichrome-stained sections from MED12 cKO hearts demonstrates interstitial fibrosis in cKO sections, absent from CTL samples. Scale bar, 50μm.
(D) Representative electron microscopy (EM) images of 8 week-old cardiac muscle tissue in control (CTL) and mutant (cKO) mice. Magnification at 16500X.
N = 5–8. Data are represented as mean ± SEM. *P < 0.05, **P < 0.01.

Changes in contractile gene expression associated with cardiac depletion of MED12

To more thoroughly analyze the changes that result from loss of Med12 in cardiac tissue, we performed microarray analysis on mRNA isolated from CTL and Med12-cKO whole hearts at P7. Of particular interest, microarray profiling revealed strong dysregulation of genes encoding several sarcomeric components, calcium handling proteins, and ion channels involved in excitation-contraction coupling (Figure 4.3A). These gene sets included essential structural genes, such as myosin light chains, alpha-actin, and MYH6, which encodes the alpha heavy chain subunit of cardiac myosin. Further gene ontology analysis of the transcripts demonstrated significant changes in genes known to function in cardiac muscle contraction (Figure 4.3A). Most notably, genes involved in the calcium handling pathway were among the most affected, including CaV3.2, a T-type channel encoded by CACNA1H, which is normally expressed in embryonic hearts and is down-regulated after birth (Yasui et al., 2005), ryanodine receptor 2 (Ryr2), Atp2a2/SERCA2, potassium voltage-gated channel KCNE1, phospholamban, all of which were down-regulated in Med12-cKO pups compared to control littermates. Up-regulated genes included tropomyosin beta (Tpm2) and calsequestrin (Casq1), both of which encode skeletal muscle-specific proteins. Acta1,

encoding the skeletal muscle-specific α-actin isoform, was also strongly up-regulated in the cardiac tissue of the Med12-cKO mice (Figure 4.3C).

Ingenuity Pathway Analysis (IPA) grouped the genes according to common ontologies and indicated that four signaling pathways were most strongly affected from this genetic dysregulation (Figure 4.3B). These signaling pathways included calcium handling, RhoA signaling, adherens junction, and actin cytoskeleton signaling.

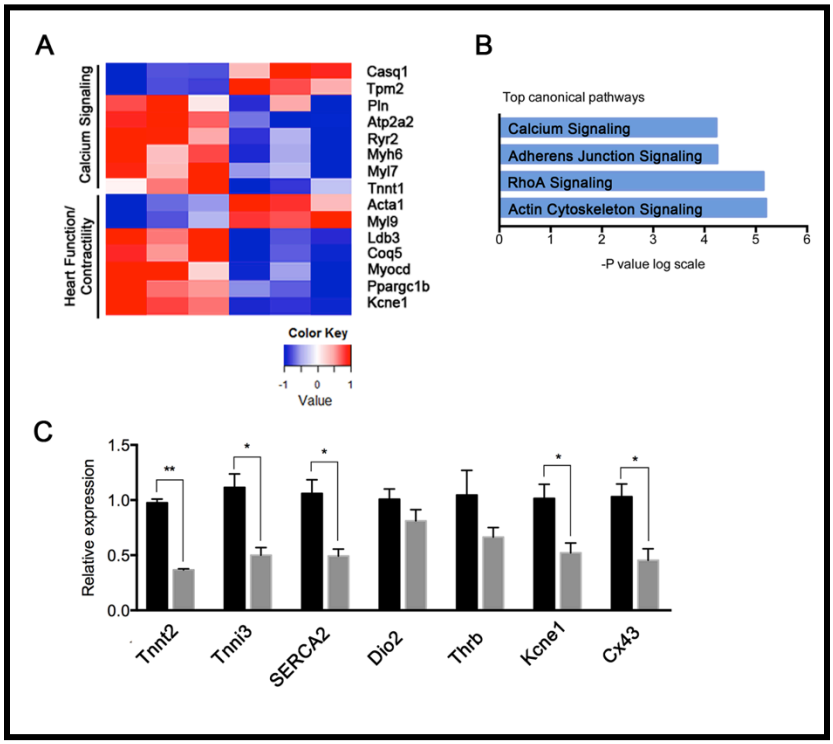

Figure 4.3. Microarray and Gene Ontology Analysis of Med12 cKO Cardiac Tissue.
(A) Heat map of hierarchical clustering of selected up- or –down-regulated genes between 1 week-old Med12-cKO and CTL littermates.
Data are presented as Z-scores of the gene expression measurements, which were used for the clustering. The heat maps represent 3 biological replicates for each genotype.
(B) Ingenuity Pathway Analysis (IPA) showing the top gene networks in Med12-cKO mice Differentially expressed genes from the Illumina Microarray analysis comparing whole heart tissue of 1-week-old neonatal mice.
(C) Real-time qPCR analysis of cardiac genes involved in cardiac electrophysiology, contractility, and Ca^{2+} handling. Realtime data are represented as ± SEM. *P < 0.05, **P < 0.01.

Cardiomyocytes lacking Med12 have enhanced calcium handling

Based on the robust changes in contractility and calcium handling gene expression observed in whole heart tissue, we expected isolated cardiac myocytes to display altered Ca^{2+} kinetics at the cellular level. Ventricular myocytes were isolated from Med12-cKO and CTL adult hearts via described methods and immediately analyzed. Upon morphological examination, isolated Med12-cKO cardiomyocytes were significantly longer than CTL, and though there was no significant difference in the diameter of the cells (Figures 4.4A and 4.4B), they had a significantly larger cell capacitance compared with CTLs, indicative of a hypertrophic phenotype. We then assessed ventricular myocytes for Ca^{2+} cycling parameters under room temperature conditions at a stimulation frequency of 0.5 Hz.

Analysis of Ca^{2+} transients from isolated cardiac myocytes indicated no alteration in baseline cytosolic $Ca2^{2+}$ levels in Med12-cKO cardiomyocytes, but the amplitude of the Ca^{2+} signal was significantly increased (Figure 4.4C and 4.4D) compared to CTL controls. The rate of Ca^{2+} decay was also significantly faster (Figure 4.4D), indicative of enhanced SR function. This discord between the contractile function assessed in isolated myocytes and intact hearts suggests that intercellular coupling between Med12-cKO myocytes may be compromised, and thus, unable to efficiently transduce mechanical forces generated at the cellular level to multicellular preparations. This finding prompted us to examine the expression levels of connexin43 (Cx43), the predominant component of gap junctions in cardiomyocytes and important in intercellular communication. Cx43 mRNA transcripts were found to be significantly down-regulated in our microarray

analysis, and this finding was further validated through qPCR from adults (Figure 4.3C). Alterations in Cx43 expression levels have been linked to arryhthmogenesis in cardiac muscle, as well as conduction abnormalities and heart failure (Saffitz and Yamada, 1998).

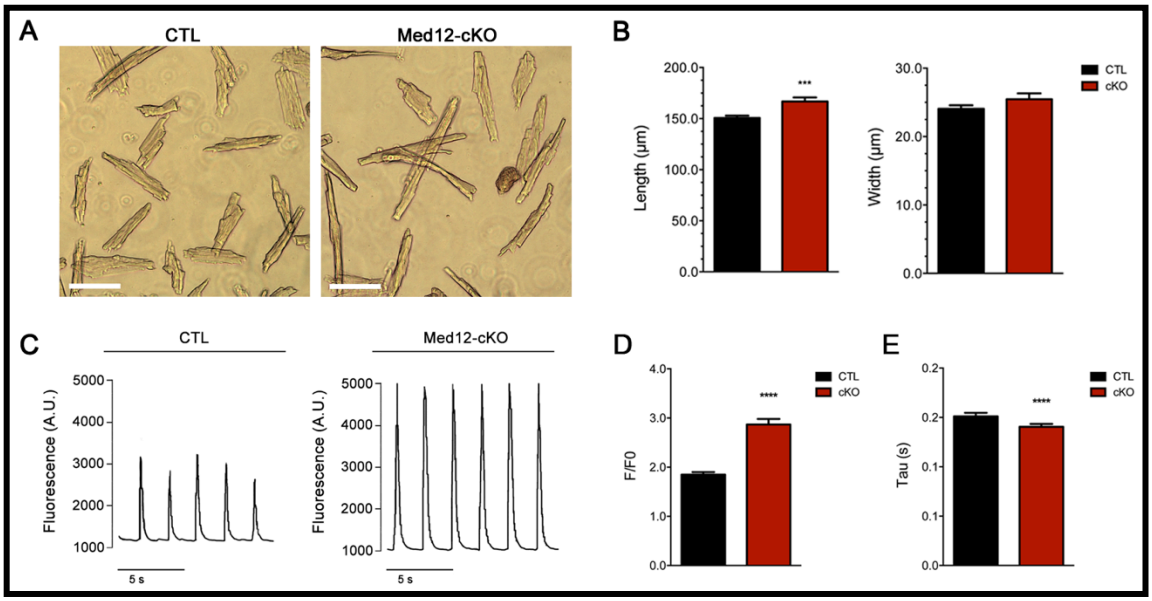

Figure 4.4. Morphological and Functional Characterization of Isolated Med12-cKO Cardiomyocytes.
(A) Cardiomyocytes were isolated from 10 week-old adult littermates using the Langendorff perfusion method. Scale bar, 100µm.
(B) Quantification of isolated cardiomyocyte length and width.
(C) Fluo-4 AM fluorescence (A.U.) intensity of single cardiomyocytes, representative of [Ca2+]i.
(D) Peak calcium amplitude as F/F0.
(E) Calcium decay rate measured in seconds.
Data are represented as ± SEM. ***P < 0.001, ****P < 0.0001. N=3.

Though individual myocytes may function with enhanced Ca^{2+} handling, electrical uncoupling at gap junctions can lead to conduction abnormalities. To observe in vivo cardiac electrical conductivity, we performed electrocardiography (ECG) on 6-week

adult Med12-cKO and CTL littermates. Through this examination we found that Med12-cKO mice displayed significantly longer QRS duration (2.13-fold) than their Cre-negative counterparts (Figure 4.5A and 4.5B), indicative of a defect of the cardiac electrical conduction system.

Figure 4.5. Deletion of Med12 from Cardiomyocytes affects the Conduction System
(A) Representative electrocardiography tracings of 6-week old male littermates.
(B) Quantification of ECG profile QRS length.
N=3-4. Data are represented as ± SEM. *P < 0.05.

Discussion

In this work, we demonstrate a novel role for the Mediator subunit MED12 in postnatal heart development and cardiac function. We show that mice lacking MED12 in cardiac muscle display significantly decreased contractility due to dilated cardiomyopathy manifesting early after birth, and modulated calcium handling in response to electrical stimulation. These changes may result, at least in part, from dysregulated transcriptional activity for genes encoding components of the contractile apparatus and calcium storage machinery.

Our results show that MED12 is essential for normal growth and morphogenesis of the heart. Cardiac deletion results in decreased ventricular contractility and dilated right and left ventricles. These defects appeared to be superficially similar to many known congenital heart abnormalities including DCM and ARVC. However, histological analysis at the cellular level showed no infiltration of fat in the Med12-cKO mutant, suggesting that the phenotype may be more closely resembling DCM than ARVC.

Additionally, we observed abnormalities in gene expression resulting from Med12 Several down-regulated genes have mutations previously reported as associated with DCM, including Myh6, Myh7, Tnnt2, Tnni3, Ldb3, Ryr2, phospholamban, and Kcne1 (Hershberger et al., 2013).

SERCA expression, which is suppressed in Med12-cKOs, determines the extent of Ca^{2+} release and ATP-consuming reuptake by the SR during the relaxation-contraction cycle. It is essential for fast muscle relaxation (Salvatore et al., 2014). Thus, Med12 regulates both sarcomeric and calcium regulatory components that may contribute to the contractile properties of the heart. As a number of genes involved in the calcium-handling pathway of cardiomyocytes were down-regulated, we hypothesized that intracellular calcium signaling would be impaired, consistent with the contractility defect we observe in vivo. Interestingly, though, calcium transient analysis in individual cardiomyocytes suggested enhanced E-C coupling. While this result was unexpected, it could be explained by the decreased mRNA expression of phospholamban, which would result in increased rates of SR Ca^{2+} transport and higher SR Ca^{2+} load, leading to increased rates of relaxation and increased force of contraction, respectively.

Most strikingly, relatively few genes on the microarrays of αMHC-Med13 TG and Med12-cKO overlapped between the two sets of significantly dysregulated transcripts, suggesting that MED13 and MED12 have differing roles in transcriptional regulation within the heart, or that perhaps the phenotype resulting from MED12 deletion overshadows the phenotype associated with MED13 deletion. Though mRNA levels of all of the kinase module subunits were unchanged (data not shown), we were unable to test whether MED13 was expression was altered at the protein level, due to technical issues. We were able to probe for CDK8 protein levels, and found them to be unchanged (data not shown). Together, this suggests that within the same tissue, two ubiquitous Mediator subunits in the same kinase module can display completely different roles from one another. However, further investigation is required to determine the mechanism by which MED12 regulates these specific sets of cardiac genes.

Methods

Generation of αMHC-Cre-Med12 cKO mice. Mice conditionally targeted at the Med12 locus ($Med12^{fl/fl}$) were provided by Heinrich Shrewe, Ph.D., of the Max-Planck Institute for Molecular Genetics (Rocha et al., 2010a). Conditional knockout alleles were generated through insertion of loxP sites flanking Exons 1-7. Heart-specific Cre-mediated excision was performed through breeding female animals homozygous for floxed Med12 alleles, with male transgenic mice expressing one allele of Cre recombinase driven by the αMHC promoter.

Histologic analysis of Med12 cKO hearts. Whole hearts were fixed with 4%PFA/PBS and processed by the UTSW Molecular Pathology Core for paraffin embedding, sectioning, and hematoxylin and eosin staining, as well as Gomori-trichrome staining, according to standard procedures (Shelton et al., 2000).

Electron microscopy. Left and right ventricular heart tissue was minced and fixed in 2% paraformaldehyde, 2.5% glutaraldehyde, and 0.1 M cacodylate buffer, prepared according to standard protocol; and electron microscopy was performed at the University of Texas Southwestern Molecular and Cellular Imaging Facility using a Tecnai G2 Spirit 120 KV TEM.

Immunohistochemistry. Tissue samples were fixed in 4% paraformaldehyde/PBS and embedded in paraffin for sectioning. Deparaffinized sections were permeabilized with 0.1% Triton-X/0.1% sodium citrate, then blocked in 2% bovine serum albumin/2% normal goat serum in PBS. Antibodies used for immunostaining were as follows. Anti-PH3 (Millipore), anti-Troponin T (Thermo, MA5-12960), and anti-Laminin (Sigma, L9393) were used in primary staining at 1:100. Anti-rabbit Alexa Fluor® 488 and anti-mouse Alexa Fluor® 555 conjugate antibodies were used for secondary staining at 1:400. Wheat-germ agglutinin Alexa Fluor® 488 was used at a concentration of 50μg/mL. TUNEL staining was performed with the Roche In Situ Cell Death Detection TMR Red Kit according to manufacturer's instructions.

Transthoracic echocardiography. Echocardiography was performed on male littermates at various stages of postnatal development, including neonates at P3 and P6, and weaned animals at 6, 8, 10, and 12 weeks of age. Cardiac function was evaluated by two-dimensional transthoracic echocardiography on conscious mice using a Vevo2100 (VisualSonics) imaging system. Neonates were kept on a heating pad prior to the procedure to avoid a vagal response. The largest anteroposterior diameters in diastole and systole were assessed in at least three recorded M-mode tracings and LV fractional shortening calculated according to the formula FS(%) = [(LVIDd − LVIDs)/LVIDd] × 100. All measurements were performed by a single experienced operator blinded to the mouse genotypes.

Isolation of adult murine ventricular cardiomyocytes. Cardiac myocytes (CM) isolated for area measurements and calcium transient analysis were taken from 8-week old males CTL and Med12-cKO mice using Langendorff perfusion. Mice were first injected intraperitoneally with 100 units of Heparin (0.1mL of 1000U/mL) and then anesthetized with 3% isoflurane. Excised hearts were immediately mounted on a steel cannula through the aorta and subjected to retrograde perfusion with Ca^{2+}-free Tyrode's solution buffer followed by enzymatic digestion by Liberase DH (Roche). Isolated myocytes were plated on laminin-coated glass coverslips, and the Ca^{2+} concentration of the buffer was increased incrementally (0.025, 0.125, 0.15, 0.175, 0.2 mmol/L), with 10 minutes of exposure at each concentration. The final Ca^{2+} buffer was then aspirated and

replaced with fresh Tyrode's-based exchange solution containing 0.2 mM $CaCl_2$ and 1% BSA.

Ca^{2+} Imaging in Ventricular Myocytes. Myocytes were loaded with 5-10 μM Fluo-4 AM (Molecular Probes) for 15 minutes to measure intracellular calcium concentration ($[Ca2+]_i$). Coverslips were mounted on the stage of an inverted microscope and perfused with normal physiological Tyrodes solution. Myocytes were paced at 0.5 Hz with a 25mA stimulation protocol and transients were recorded at 75 frames/second with an Andor iXon Ultra 897 back-illuminated EMCCD camera and a 20X objective. F0 (or F unstimulated) was measured as the average fluorescence of the cell 50 ms prior to stimulation. The maximal Fluo-4 fluorescence (F) was measured at peak amplitude. All data analysis was performed using pClamp8 software (Molecular Devices).

Gene expression analysis. Whole hearts were cleared of blood in PBS prior to being flash frozen in liquid nitrogen, and total RNA was isolated following tissue homogenization in Trizol (Invitrogen) according to manufacturer's instructions. cDNA was generated by reverse transcription using random hexamer primers (Invitrogen). Gene expression was measured by quantitative real time PCR either with purchased gene specific Taqman probes (ABI) or primers designed (see appendices) for SYBR green qPCR. Data was normalized to 18S expression.

Microarray analysis. Individual triplicate samples of P7 male CTL and Med12-cKO whole heart total RNA were analyzed on an Illumina MouseWG-6 v2.0 BeadChip. Relative fold change was then calculated by comparison of signal intensities. Fold changes greater or less than 1.4-fold were subject gene ontology analysis (Ingenuity Systems) with a statistical threshold of p=0.05.

Electrocardiography. 6-week old littermates were anesthetized with 1.5% isoflurane and placed on a heating pad. Body temperature was maintained and controlled by a rectal probe. Two electrodes were placed subcutaneously in the right axillary area and the left lower abdomen of mice. ECG leads were recorded directly using two ECG amplifiers connected in series to a data acquisition unit. 10-minute ECG strips were recorded (2000 data points per second) and displayed using data acquisition software (LabChart, ADInstruments). The QRS duration was directly measured using an on-line caliper.

CHAPTER V

REGULATION OF SKELETAL MUSCLE GENE EXPRESSION AND PERFORMANCE BY MED12

Introduction

Skeletal muscle constitutes an estimated 40% of total human body mass in an average healthy individual (Rolfe and Brown, 1997). Skeletal muscle is heterogeneous, composed of fast and slow-twitch fiber types. These fiber types differ in composition of contractile proteins and oxidative capacity, thus displaying contrasting contractile and metabolic properties. Additionally, muscle fiber type content of a specific muscle group can be modified in response to metabolic or mechanical stress. Within skeletal muscle, proper sensing and propagation of mechanical forces requires the coordination of multiple cytoplasmic and nuclear components. To determine the function MED12 in developing skeletal muscle, we conditionally deleted the Med12 gene in mice by using skeletal muscle-specific transgenes driving Cre recombinase. Mice lacking skeletal muscle expression of Med12 displayed severe muscle myopathy in diaphragm tissue, and were characterized overall by a deficiency in muscle growth. These findings reveal an essential role for MED12 in the control of muscle fiber growth and development.

Results

Skeletal muscle-specific deletion of MED12 causes postnatal lethality due to failure to thrive

To enable the skeletal muscle-specific depletion of Med12, we bred female Med12fl/fl animals to transgenic males in which Cre recombinase expression was controlled by the mouse *myogenin* promoter and the enhancer of the mouse *MEF2C* gene, regulatory elements which both are active only in the skeletal muscle lineage from E8.5 at adulthood (Li et al., 2005).

Though we observed expected Mendelian ratios of Med12-mKO mice immediately at birth, genotyping of offspring from myo-Cre+ males and Med12fl/fl female crosses revealed that ~40% of male Med12-mKO neonates died within the first 24 hours after birth. A range of phenotypic severity was observed in P1 animals, suggesting the loss of mutant mice immediately after birth likely represents those with more acute myofibrillar disarray. In the Med12-mKO mutants that were analyzed immediately postnatally, Med12 levels were significantly reduced (Figure 5.1A). Immediately after birth, neonatal Med12-mKO animals were found to weigh significantly less than their control littermate counterparts (Figure 5.1B and 5.1C).

Furthermore, we observed that >70% of the Med12-mKO mice died by 3 weeks of age, and of the remaining animals none survived beyond 7 months (Figure 5.1D). Adult Med12-mKO mice remained half the weight of Cre-negative Med12fl/Y control (CTL) littermates (Figure 5.2A), and exhibited dorsal kyphosis by 9 weeks of age,

demonstrating a failure to thrive (Figure 5.2B). Additionally, muscle and white adipose tissue weights from these Med12 mutants were found to be dramatically decreased compared to CTL (Figure 5.2C). Histological analysis of animals at several postnatal time points revealed that myofiber size was significantly smaller by cross-sectional area (CSA) (Figure 5.2D and 5.2E).

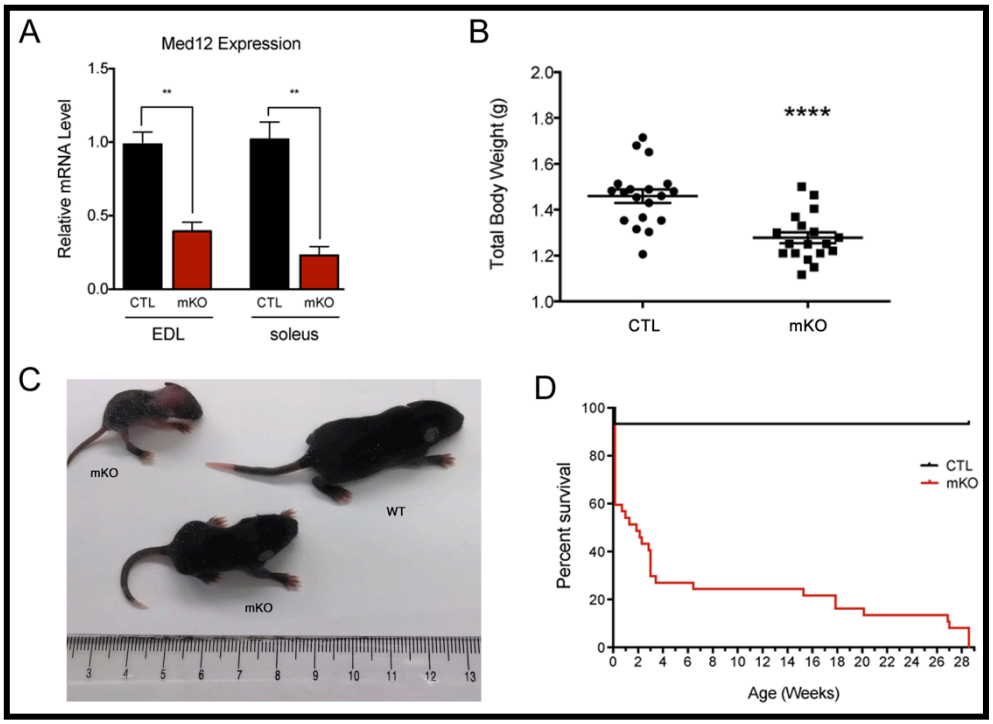

Figure 5.1. Skeletal muscle-specific deletion of MED12 causes postnatal lethality.
(A) Med12 mRNA levels in skeletal muscle of CTL and Med12-mKO 12-week old adult mice were detected by real time PCR.
(B) Total body weights of P1 males (N = 15 CTL, N = 11 mKO).
(C) Representative image of CTL mouse with two Med12-mKO littermates at P10, demonstrating variability of runted morphology.
(D) Kaplan-Meyer curve showing percentage survival of mKO animals (N = 45 animals for each genotype).
Data are represented as mean ± SEM. **P < 0.01, ****P < 0.0001.

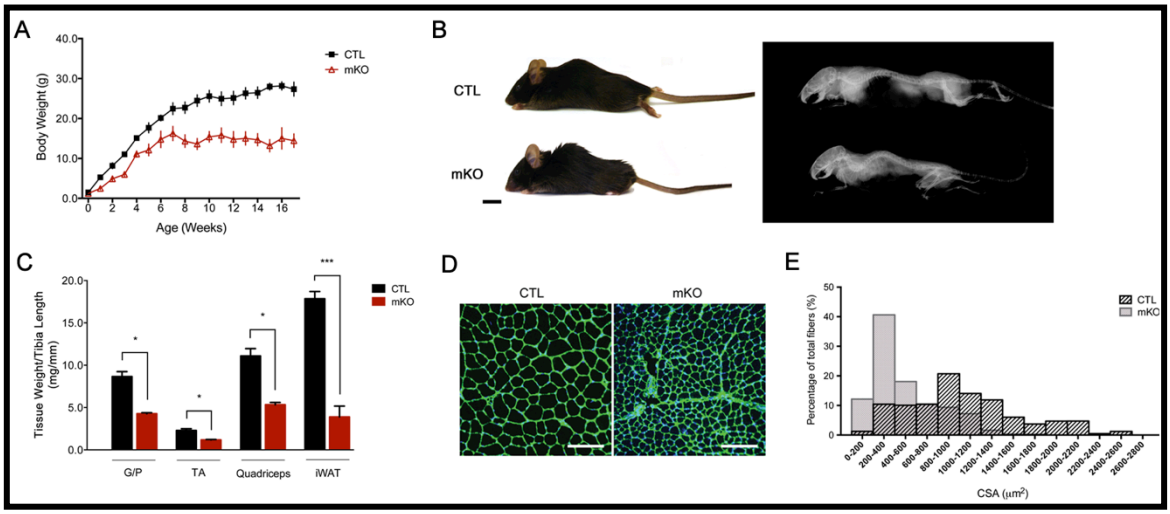

Figure 5.2 Med12-mKO mice exhibit dramatically reduced body weight and fail to thrive
(A) Growth curve analysis of surviving Med12-mKO mice as compared to control littermates.
(B) Comparative x-ray images of adult animals. Scale bar represents 1cm.
(C) Ratio of isolated tissue mass (mg) to tibia length (mm).
(D) Fiber size in Tibialis anterior (TA) muscle indicated through laminin staining (green) in 9 wk mice. Nuclei are stained with DAPI (blue). Scale bar, 100μm.
(E) Quantification of fiber cross-sectional area (CSA), represented as percentage of total fibers counted. (n=2000-2500 fibers counted).
N=3 unless otherwise noted. Data are represented as mean ± SEM. $^{**}P < 0.05$, $^{***}P < 0.001$.

Med12-deficient skeletal muscle has abnormal structure and function

To determine whether loss of Med12 had any effect on sarcomere structure and function, we performed histologic analysis of skeletal muscles from P10 mKO mouse pups and found that sarcomeres were present in the diaphragm, but a large subset of fibers showed disorganization, with pronounced Z-line streaming and reduced intermyofiber space. The sarcomeres were out of register and their shortening was highly irregular; some were overstretched, while others were shortened maximally by about twofold, with variable range of sarcomere lengths (Figure 5.3A). Further immunofluorescence on sections from frozen tibialis anterior (TA) muscles of adult mice

revealed drastic desmin accumulation, indicative of myopathic cellular disorganization (Figure 5.3C).

To test muscle function, we measured the maximum force generated during tetanic contraction of whole hind limbs isolated from P1 mice (Figure 5.3D). For the purposes of this experiment female mice (which were not analyzed in any of other previous or subsequent experiments) were included in the data set. Due to the nature of the breeding crosses, all Cre+ females contain a Med12 fl/+ allele, generating heterozygous animals for comparative analysis. Despite the lack of observable defects in neonatal hind limb muscle by electron microscopy analysis (Figure 5.3B), P1 mKO muscle demonstrated >10% reduction in hind limb strength.

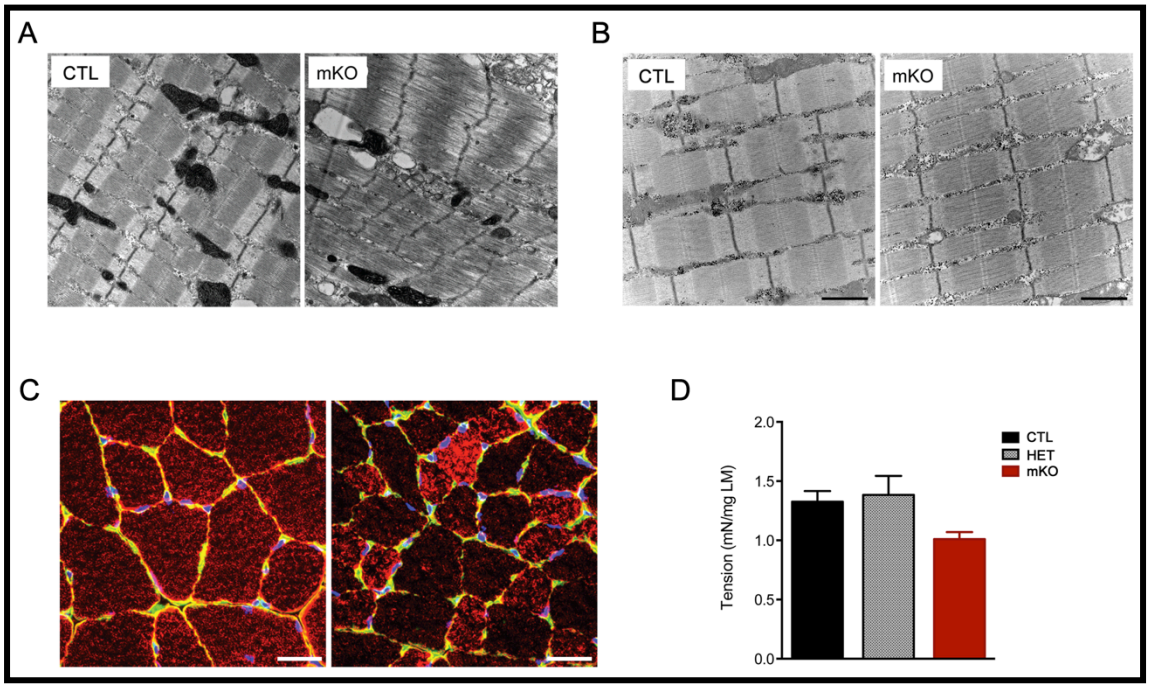

Figure 5.3. Med12-deficient skeletal muscle has abnormal structure and function
(A) Representative electron microscopy (EM) images of P10 diaphragm muscle fibers in control (CTL) and mutant (mKO) mouse pups.

(B) EM images of P10 quadriceps muscle fibers in CTL and mutant (mKO) mouse pups. Scale bar, 1μm. **(C)** Immunofluorescent images of transverse sections of TA muscle from 9 wk old control and Med12-mKO mice. Desmin (red), laminin (green), and DAPI to represent nuclei (blue). Scale bar, 20μm. **(D)** Maximum contractile force of P1 CTL, myo-Cre+ Med12fl/+ (HET), and mKO hind limb following 150-Hz stimulation, normalized to limb mass. (CTL, N = 15; HET, N = 3; and mKO, N = 7).

Loss of Med12 in skeletal muscle leads to dysregulation of several transcription factor pathways

We performed microarray analysis on the quadriceps of P1 neonatal pups and found that, in contrast to the genetic profile of the cardiac deletion mutants (Med12-cKO), a number of pathways were affected by loss of Med12 in skeletal muscle. A large fraction of the affected genes were known to be involved in musculoskeletal development, as defined by Ingenuity Pathway Analysis (IPA) of genes changed >1.3-fold in either direction (Figure 5.4A).

The microarray analysis revealed that of the 353 genes that were significantly up- or down-regulated, the top hits were involved in a number of different transcription factor pathways, such as nuclear receptor (NR) activation (including Ppargc1a, Ppargc1b, Prkaca, Slc2a1, Ucp3, and Gdf1), glucocorticoid (GR) receptor signaling (such as Adrb2, Nfkbia, and Nfkb1), and Wnt/β-catenin signaling (Axin2, Wnt5a, Wnt4, Pitx2) (Figures 5.4D and 5.4G). Also among the most dysregulated were a number of genes involved in calcium handling and contractility, though these genes did not overlap with the gene sets from the cardiac deletion analysis (Figures 4.4E and 5.4).

Further Ingenuity Pathway Analysis (IPA) was used to identify relationships among genes and place them into functional categories. These analyses revealed that

cellular growth and proliferation, cell death and survival, gene expression, and cell signaling were prominently changed in muscle from neonatal Med12-mKO mice (Figure 5.4E). As illustrated in the Venn diagram, most of these grouped genes fell into multiple categories (Figure 5.4F).

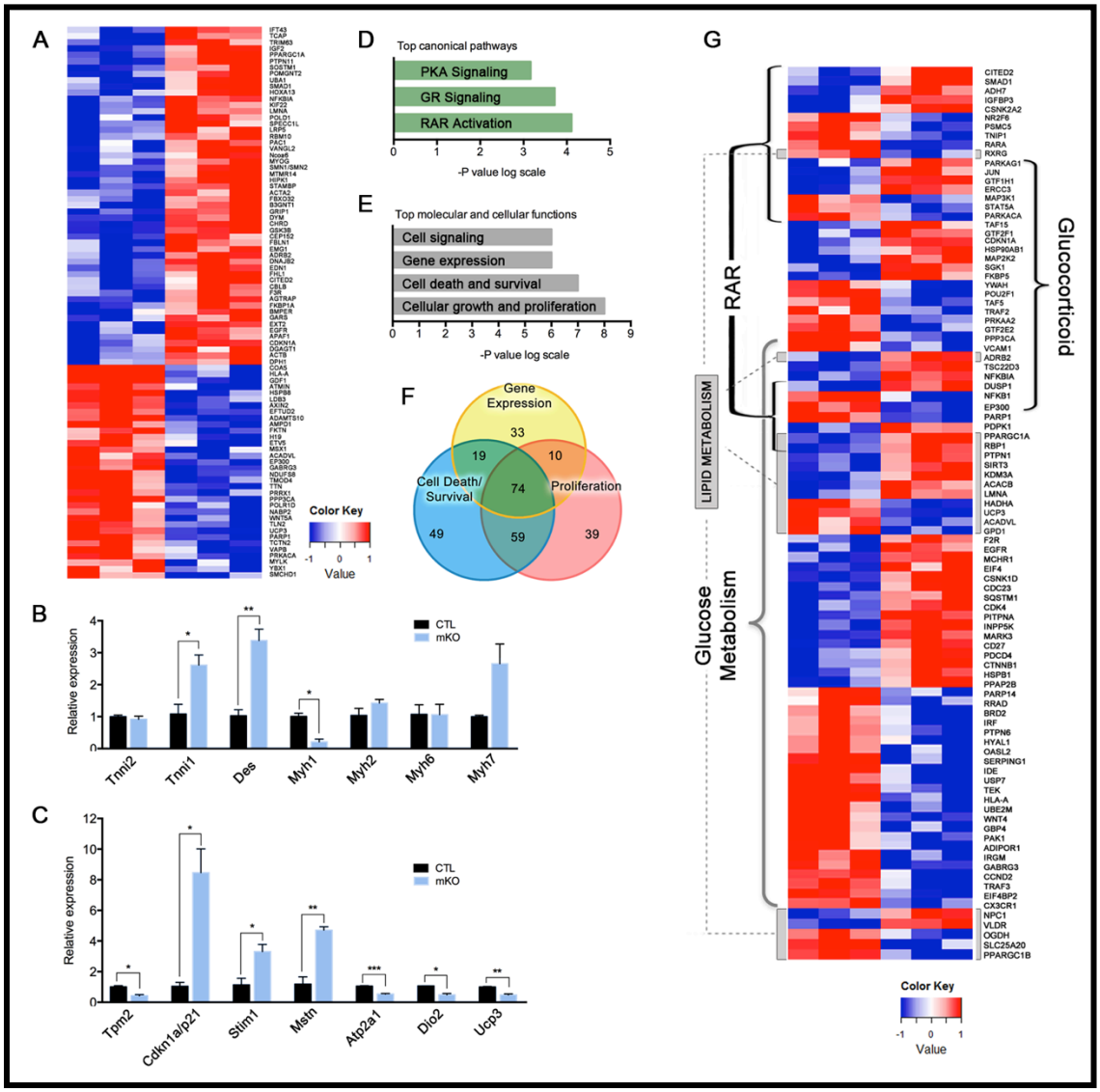

Figure 5.4. Transcriptional, metabolic, and growth pathways modified by MED12 deletion in skeletal muscle

(A) Heat map of hierarchical clustering of selected up- or down-regulated genes involved in musculoskeletal development between neonatal Med12-mKO and CTL male littermates, according to Ingenuity Pathway Analysis.
(B) Real-time PCR analysis to validate mRNA expression levels of genes encoding structural and sarcomeric proteins in adult Med12-mKO mice.
(C) Real-time PCR analysis to validate gene expression levels involved in contractility, calcium handling, and metabolism in adult Med12-mKO mice.
(D) Ingenuity Pathway Analysis (IPA) showing the top gene networks in Med12-mKO mice Differentially expressed genes from the Illumina Microarray analysis comparing quadriceps tissue of P0.5 neonatal mice.
(E) Microarray analysis (via IPA) revealed top molecular and cellular functions of differentially expressed genes in neonatal CTL and Med12-mKO mouse quadriceps tissue.
(F) Venn diagram showing overlap of top cellular and molecular functions affected and the number of genes from the microarray that fall into each category.
(G) Heat map of hierarchical clustering of selected up- or down-regulated genes involved in multiple metabolic pathways in neonatal Med12-mKO and CTL male littermates.
Heat map data are presented as Z-scores of the gene expression measurements, which were used for the clustering. The heat maps and array data represent 3 biological replicates for each genotype.
Real-time data are represented as mean ± SEM. *P < 0.05, **P < 0.01. n=3.

Med12-deficient skeletal muscle exhibits failure to hypertrophy

We assessed the effect of MED12 deletion on myotube growth, we first isolated primary myoblasts from control (Med12fl/Y) mice according to previous methods (Rando and Blau, 1997). After purifying the cultured population through pre-plate passaging, the myoblasts were subjected to differentiation medium. After 48 hours, the myotubes were transduced with Ad-GFP or Ad-CreGFP (Med12 deleted) adenoviruses; 48 hours later they were treated or not with recombinant IGF1 (rIGF1) for an additional 48 hours. We observed that IGF1 treatment of myotubes lacking Med12 did not display an increase in myotube diameter (Figures 5.5A and 5.5B). This suggests that MED12 is required for IGF1-induced hypertrophy in culture.

To further investigate the role of Med12 in skeletal muscle hypertrophy, compensatory hypertrophy (CH) of the plantaris muscle was performed in HSA-Cre-ER^{T2};Med12fl/Y mutant mice previously tamoxifen-injected to induce myofiber-specific Med12 loss. In addition, control and mutant mice were injected with tamoxifen during

the CH procedure. Efficient Med12 loss was achieved at the transcript level (Figure 5.5C). No obvious differences in muscle mass, myofiber cross-sectional area (CSA), and myofiber number were observed between control and mutant plantaris muscles before overload (Figures 5.5D). In this muscle growth model, we observed a significant increase in muscle mass and myofiber CSA of control muscles 21 days after overload (Figure 5.5E). In contrast, growth was completely blunted in mutant muscles (Figures 5.5E and 5.5F), showing that Med12 is necessary for overload-induced myofiber hypertrophy.

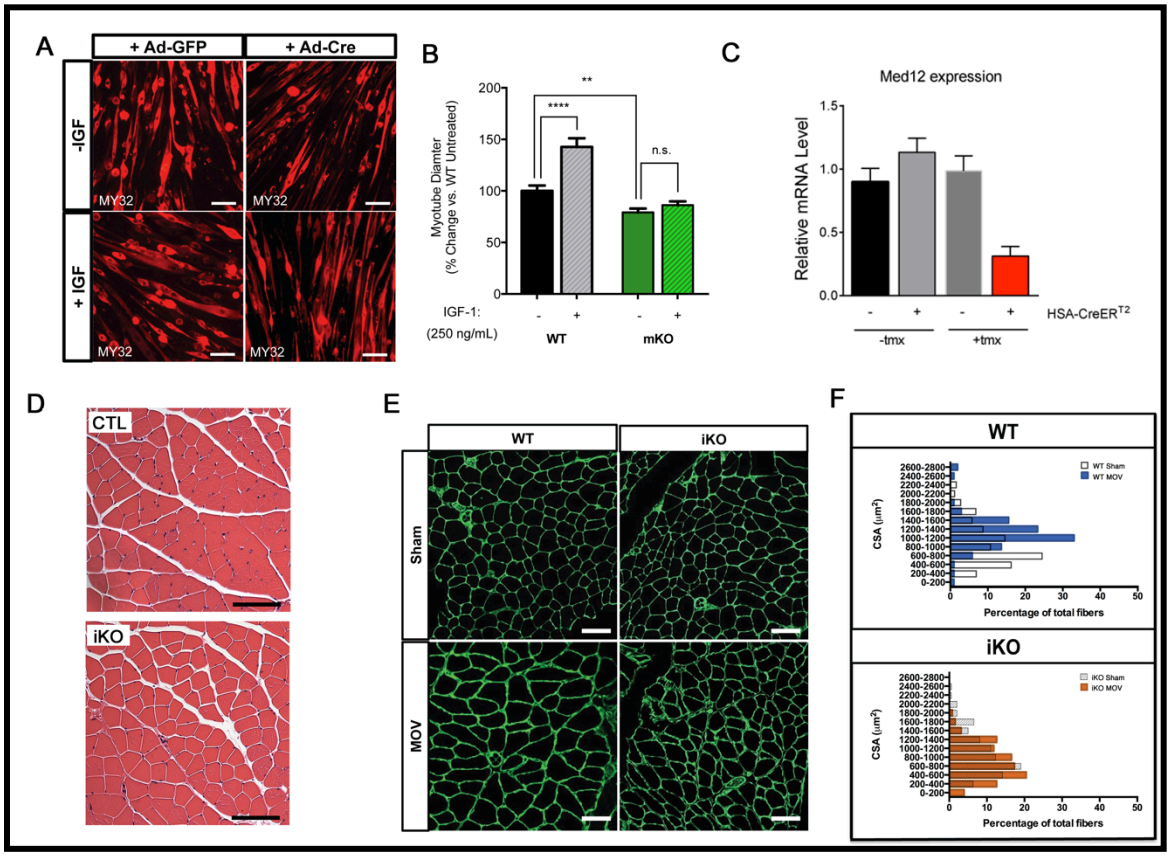

Figure 5.5. Med12-deficient skeletal muscle exhibits failure to hypertrophy
(A) MY32 staining of Med12-floxed cultured primary myotubes that have been differentiated for 96 hours, treated or untreated with recombinant IGF-1 (250 ng/mL). Scale bar, 100 μm.
(B) Quantification of myotube diameter, represented as percent change vs. WT untreated cultures.

(C) Med12 mRNA levels in skeletal muscle of CTL and Med12-iKO adult mice were detected by real time PCR.
(D) H&E stained transverse sections of myofibers. Scale bar, 100 μm.
(E) Laminin staining of plantaris muscles of tamoxifen-induced Med12 mutant animals at 8 wks. Scale bar, 50 μm.
(F) Quantification of fiber cross-sectional area (CSA), represented as percentage of total fibers counted. (n=800-1000 fibers counted).
Data are represented as mean ± SEM. *P < 0.05, **P < 0.01, ****P < 0.0001.

Metabolic defects in Med12-mKO skeletal muscle

As we observed dysregulation of the genes in multiple metabolic pathways (Figure 5.4G), we further investigated the metabolic differences in Med12-deleted skeletal muscle. Staining of histological sections for myofiber type with metachromatic ATPase stain and immunohistochemistry against β-MHC showed a substantial increase of type I myofibers in the soleus of Med12-mKO mice (Figures 5.6A and 5.6B). Consistent with this finding, analysis of gene expression in the soleus by real-time PCR also demonstrated an induction of slow fiber-specific Myh7 expression in response to MED12 deletion (Figure 5.4B). Our results suggest the MED12 deletion is sufficient to induce a complete conversion of all fast myofibers in soleus to a slow, oxidative type I phenotype.

Upon histological examination of inguinal WAT (iWAT) depots from adult mice, we observed a sharp reduction in cell size of adipocytes, and the liver appeared overall normal in morphology (Figure 5.6C). Consistent with these findings, NMR spectrometry reveal that the difference in weight between the Med12-mKO and control groups was due not only to differences in lean mass, but also significant reduction of fat mass (Figure 5.6D). Serum glucose and triglyceride levels were also reduced at baseline in P7 animals (Figure 5.6E).

The PI3K/AKT signaling pathway has been implicated this in myocyte growth and muscle mass regulation (Rommel et al., 2001). This pathway is activated in skeletal muscle through extrinsic or paracrine IGF-1 upon binding with its receptor at the plasma

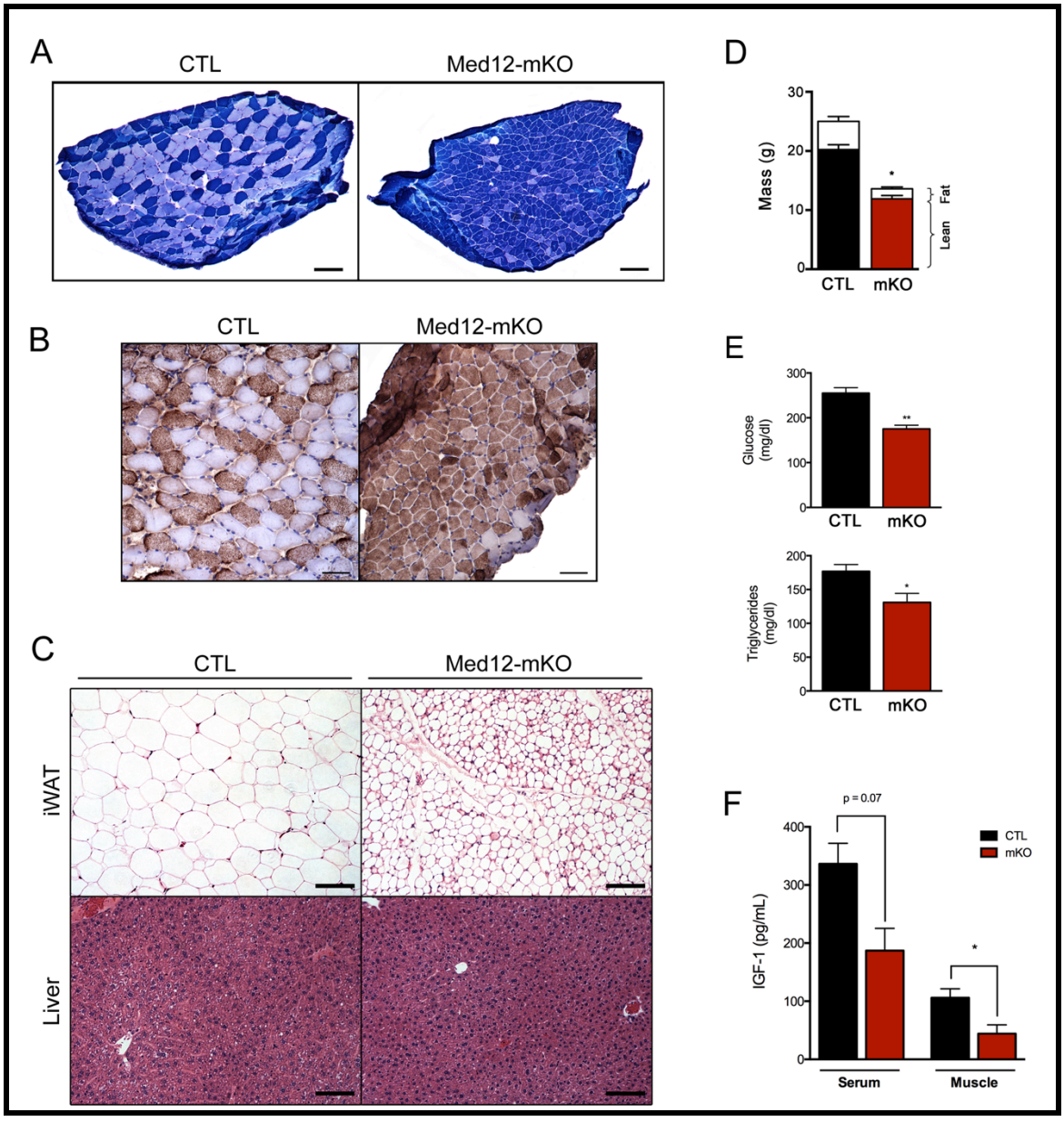

Figure 5.6 Modulation of Myofiber Metabolic Properties in Med12-Deficient Skeletal Muscle
(A) Detection of type I myofibers in soleus of control and Med12-mKO 9-wk adult mice by metachromatic ATPase staining. Scale bar, 100 μm.

(B) Immunohistochemistry for βMHC to identify type I myofibers in the soleus of control and Med12-mKO 9-wk mice. Scale bar, 50 μm.
(C) H&E stain of inguinal WAT and liver tissue from 9-wk animals. Scale bar, 50 μm.
(D) Body composition measured by NMR to determine fat mass and lean tissue mass. n=6 male 9-11-wk adults per group.
(E) Serum glucose and triglyceride levels in P7 males.
(F) ELISA detection of serum and muscle tissue IGF-1 levels in P7 quadriceps muscle.
Data are represented as mean ± SEM. *P < 0.05, **P < 0.01. N=3 unless otherwise noted.

membrane. Indeed, IGF-1 is suggested to be a major contributor to controlling skeletal muscle tissue growth (Schiaffino and Mammucari, 2011). To determine whether the Med12-mKO mice had irregular IGF-1 concentrations, we used ELISA detection to examined both circulating levels and muscle-tissue levels of IGF-1 in P7 animals. We found that skeletal muscle tissue from P7 pups contained significantly reduced IGF-1 levels, and the reduction of circulating IGF-1 detected in serum was trending toward significant levels ($P = 0.07$). As disrupted expression of muscle-specific IGF-1 receptor (IGF-IR) has been shown to phenotypically manifest as growth retardation in mouse models (Heron-Milhavet et al., 2010; Mavalli et al., 2010), this suggests that the growth deficiency we observe in the Med12-mKO mice may be due in part to reduced IGF-1 signaling in muscle, though further investigation is required.

Discussion

To determine the role of MED12 in skeletal muscle development, we deleted a conditional Med12 allele by using a two different skeletal muscle-specific Cre transgenes: one that expressed embryonically through adulthood, and one inducible transgene to bypass development. The phenotypes of these mutant mice reveal an essential role for MED12 in the control of skeletal muscle growth.

Med12-mKO animals were significantly smaller than their Cre-negative counterparts, and nearly half of the mutants died within the first 24 hours after birth. The animals that survived beyond this time point typically showed a failure to thrive, and became severely kyphotic with age. Through EM analysis, we found sarcomeric

disorganization in diaphragm muscle of mutant mice pre-weaning, suggesting that the lethality observed may be due to asphyxiation from failing diaphragm contractility. In further support of our hypothesis, microarray analysis demonstrated dysregulation of a number of genes involved contractility and calcium handling, including mRNA down-regulation of SERCA, calcineurin, and Tpm2, which belongs to the tropomyosin family that encodes proteins that bind to actin filaments and stabilize them by regulating access to actin modifying proteins. Moreover, muscle force contraction in neonatal mutants is reduced in hind limb muscles when compared to control groups and heterozygous females.

In addition to these dysregulated pathways, we also found a number of NR genes and metabolic genes changed in the muscle of neonates, which may contribute to the severity of the phenotype in Med12-mKO animals. Of note, Med13-cKO animals also displayed modulation of NR gene expression with cardiac tissue, albeit on differing gene sets, as well as altered energy metabolism (Grueter et al., 2012). Further investigation is necessary to parse out the role of MED12 in growth and its role in NR-mediated transcriptional signaling. To do this, we will further utilize our muscle-specific inducible knockout mouse line to bypass development and postnatal muscle growth, and conduct further metabolic analysis on these animals, which have already demonstrated a role for MED12 in compensatory muscle hypertrophy.

The diverse gene sets affected by MED12 deletion in skeletal muscle may suggest that MED12 is required for transcriptional regulation of multiple pathways, or may modulate transcriptional activity of other master regulators involved in many aspects of

muscle development. For example, MED13 is suggested to modulate TH signaling in cardiac tissue, which has been shown to affect calcium regulatory components that contribute to the contractile properties of cardiomyocytes, as well as postnatal growth (Salvatore et al., 2014). In wild-type animals, the levels of TH in plasma increase immediately after birth in rodents, and the capacity of skeletal muscle to increase the intracellular concentrations of T3 is also high during this period, along with Type II iodothyronine deiodinase (DIO2) activity (Salvatore et al., 2014). In the absence of TH in skeletal muscle, the switch from expression of neonatal MYH isoforms to adult MYH isoforms is delayed or incomplete, and SERCA1a fails to increase (Schiaffino and Reggiani, 2011). It would be interesting to test further if TH signaling is altered in our Med12-mKO animals, which may in turn account for the array of transcriptional pathways affected.

Methods

Generation of myo-Cre-Med12 (mKO) mice. Skeletal muscle-specific Cre-mediated excision was performed through breeding homozygous Med12fl/fl females with male transgenic mice expressing one allele of Cre recombinase driven by a Mef2c skeletal muscle enhancer and a minimal myogenin promoter (myo-Cre) as previously described (Li et al., 2005).

Inducible HSA-Cre-ER^{T2}-Med12 (iKO) mice. For inducible skeletal muscle-specific Cre-mediated excision in adults, homozygous Med12fl/fl females were bred with male

transgenic mice expressing one allele of the tamoxifen-inducible Cre-ER^{T2} recombinase driven by a 2.2-kb genomic segment of the human skeletal muscle α-actin promoter (HSA-Cre-ER^{T2}) as previously described (Schuler et al., 2005).

NMR. Male mouse body composition parameters including fat mass, lean tissue mass and water were analyzed using a Bruker Minispec mq10.

Histologic analysis of Med12 mKO muscle. Whole muscle tissues were fixed with 4% paraformaldehyde (PFA)/PBS for 48 hours and processed by the UTSW Molecular Pathology Core for paraffin embedding, sectioning, and hematoxylin and eosin staining using standard procedures (Shelton et al., 2000).

Electron microscopy. Quadriceps and diaphragm tissue was minced and fixed in 2% paraformaldehyde, 2.5% glutaraldehyde, and 0.1 M cacodylate buffer, prepared according to standard protocol; and electron microscopy was performed at the University of Texas Southwestern Molecular and Cellular Imaging Facility using a Tecnai G2 Spirit 120 KV TEM.

Fiber-type staining. Soleus, GP, TA, and EDL muscles were isolated at 9 weeks of age and were embedded in a 3:1 ratio of Tissue Freezing Medium to gum tragacanth. Samples were flash frozen and sectioned on a cryostat-microtome. Metachromatic ATPase staining was performed as previously described (Ogilvie and Feeback, 1990).

Immunohistochemistry. Frozen tissue samples were fixed in 4% paraformaldehyde and permeabilized with 0.1% Triton-X, then blocked in 2% bovine serum albumin/4% normal goat serum in PBS. Antibodies used for immunostaining were as follows. Anti-Desmin (Dako, Clone D33) and anti-Laminin (Sigma, L9393) were used in primary staining at 1:100. Anti-rabbit Alexa Fluor® 488 and anti-mouse Alexa Fluor® 555 conjugate antibodies were used for secondary staining at 1:400. Wheat-germ agglutinin Alexa Fluor® 488 was used at a concentration of 50μg/mL. For fiber type detection, Tissue samples were fixed in 4% paraformaldehyde and embedded in paraffin for sectioning. Deparaffinized sections were permeabilized with 0.04% Pronase E, then blocked in 0.5% bovine serum albumin/5% normal goat serum in PBS. NOQ7.5.4D (1:16000) was used for primary detection of Type I myosin, and HRP-conjugated secondary (Sigma, A8924) followed by DAB chromagen reaction were used for detection. Samples were then counterstained with hematoxylin.

Gene expression analysis. Whole skeletal muscle was flash frozen in liquid nitrogen, and total RNA was isolated following tissue homogenization in TRIzol reagent (Invitrogen) according to manufacturer's instructions. cDNA was generated by reverse transcription of total RNA using random hexamer primers (Invitrogen). Gene expression was measured by quantitative real time PCR either with purchased gene specific Taqman probes (ABI) or primers designed (see appendices) for SYBR green qPCR. Data were normalized to 18S expression.

Quantification of myofiber size and number. Frozen sections were fixed in 4% PFA and stained with Alexa488-conjugated wheat germ agglutinin (Invitrogen) at a concentration of 50μg/mL. Fiber cross-sectional area wad measured using ImageJ software.

Microarray analysis. Individual triplicate samples of total RNA from CTL or Med12-mKO P1 pooled quadriceps were analyzed on an Illumina MouseWG-6 v2.0 BeadChip. Relative fold change was then calculated by comparison of signal intensities. Fold changes greater or less than 1.3-fold were subject gene ontology analysis (Ingenuity Systems) with a statistical threshold of p=0.05.

Neonatal muscle contraction. P1 pups were placed in a weigh boat on wet ice for 15 minutes then euthanized by decapitation, and hind limbs were then skinned. Non-absorbable braided silk suture (6-0) was tied proximal to the knee and the intact hind limb was severed at the hip. The preparations were placed in an incubated 30°C oxygenated (95% O_2, 5% CO_2) physiological salt solution (PSS) (Wolff et al., 2006). The foot was placed in a clamp at the base of the bath and the suture tied to arm of a dual-mode servomotor system (300B, Aurora Scientific, Inc). Resting tension was maintained by a stepper motor (Wolff et al., 2006). Data were obtained and analyzed with Dynamic Muscle Control (DMC v.4.1.6,), and Dynamic Muscle Analysis (DMA v.3.2) software, respectively (Aurora Scientific, Inc.). Optimal conditions for activation of the hind limb

muscles were determined as follows: twitch responses were elicited to determine the optimal resting tension (i.e., optimal length) (0.25, 0.50, 0.75, and 1.0g); the optimal voltage (15, 20, 25, 30, 35, 40V) and the optimal pulse width (250, 500, 750ms). Optimal values used thereafter were 0.5g, 30V, and 500ms, respectively. Following initial twitch and tetanic contractions, data are reported for 150Hz contractions as normalized stress (mN/mg limb mass). Experiments were performed double-blinded with genotyping analyzed following acquisition of data. Animal procedures were approved by the Institutional Animal Care and Use Committee at UT Southwestern Medical Center and Virginia Tech.

Induction of compensatory muscle hypertrophy by mechanical overload. Animals were anesthetized with tribromoethanol (Avertin) at 250mg/kg, intraperitoneally), and mechanical overload (MOV) of plantaris muscles was induced by surgical section of the distal tendon of the medial and lateral gastrocnemius muscle, the distal portion of which was excised. The incision was then sutured with resorbable thread. This procedure induces muscular compensatory hypertrophy as a response to functional overloading in the plantaris and soleus muscles. Sham-operated limbs were used as controls. 21 days post-surgery, animals were sacrificed and muscles were dissected and flash-frozen for sectioning and histological analysis. All animal procedures were approved by the Institutional Animal Care and Use Committee at UT Southwestern Medical Center.

Primary cell culture. Primary myoblasts were isolated from control (Med12fl/Y) neonatal mice according to previous methods (Rando and Blau, 1997). Pre-plating was used to purify the cell population and remove fibroblasts. Primary myoblasts were grown in growth medium (GM, Ham's F10 media supplemented with 20% fetal bovine serum and 5 ng/ml bFGF) on laminin-coated dishes. Medium was changed daily and cultures were passaged at 60-70% confluence. To induce myotube formation, GM was replaced with differentiation medium (DM) composed by DMEM supplemented with 2% horse serum, for 48 h. The differentiated myotubes were then transduced with Ad-GFP or Ad-CreGFP adenoviruses; 48 hours later they were treated or not with 250ng/mL recombinant IGF1 (R3 IGF-I human, I1271Sigma) for an additional 48 hours. All media were supplemented with 100 U/ml penicillin and 100 µg/ml streptomycin.

Measurement of serum and tissue biomedical markers. With a 6-hr fast, P7 male mice were sacrificed by rapid decapitation to avoid stress response, and blood samples were immediately collected into K+EDTA tubes with centrifugation-separated plasma stored at $^{-}$80ºC until assayed. Quadriceps tissues were isolated and homogenized in PBS according to tissue weights. Serum concentrations of insulin-like growth factor-1 (IGF-1) were quantified using ultrasensitive mouse enzyme-linked immunosorbent assay (ELISA) kit (R&D Systems), according to manufacturer's instructions. For glucose and triglyceride detection, calorimetric assays were used (Wako, Pointe Scientific). Absorbance measured at 520 nm using SoftMax Pro software/plate-reader.

Immunocytochemistry. Primary myoblast and myotube cultures were washed with PBS, followed by fixation in 4% paraformaldehyde and permeabilized with 0.1% Triton-X, then blocked in 2% bovine serum albumin/4% normal goat serum in PBS. Anti-Myosin MY32 antibody (Sigma, M4276) was used for primary detection, and anti-mouse Alexa Fluor® 555 conjugate antibodies were used for secondary staining.

CHAPTER VI

CONCLUSION AND FURTHER REMARKS

In these studies, we established that two distinct Mediator subunits of the CDK8 component modulate different sets of genes and pathways within the same tissue. Furthermore, we show that the MED12 subunit regulates expression of gene sets in a cell-type specific manner, with a broader spectrum of pathways affected in skeletal muscle than in cardiac tissue.

Interestingly, only a handful of genetic targets overlapped between the three microarrays. Med13 manipulation in cardiac tissue resulted in the down-regulation of a host of genes known to be targets of NRs, such as TR, RXR and LXR. None of these genes, however, were significantly changed in Med12-deleted cardiac tissue. Instead, the most significantly changed genes were involved in contractility, such as actins and myosins, or calcium homeostasis. Furthermore, the narrow set of genes dysregulated in Med12-cKO hearts did not, for the most part, overlap with the wide array of genetic pathways affected in Med12-mKO skeletal muscle. In fact, of the hundreds of genes that appeared on each array, 8 were found to be changed significantly in both datasets (Table 6.1).

Table 6.1 Overlapping genes from Med12 cKO and mKO microarrays

Gene	*Function*	*Fold change in cardiac muscle*	*Fold change in skeletal muscle*
FNDC5	Positive regulation of brown fat cell differentiation	↓ 0.57	↓0.81
Ppargc1b	Ligand-dependent nuclear receptor transcription coactivator activity	↓ 0.68	↓ 0.52
Ldb3	Cytoskeletal assembly; clustering of membrane proteins	↓ 0.71	↓ 0.76
Coq5	Mitochondrial protein thought to be involved in biosynthesis of CoQ10	↓ 0.71	↓ 0.64
Tpm2	Muscle contraction	↑ 3.0	↓ 0.8
VLDR	VLDL-triglyceride metabolism	↓ 0.78	↑ 1.55
GPT2	Glucose, amino acid, and fatty acid metabolism and homeostasis	↓ 0.73	↑ 1.32
SLC4A3	Chloride/bicarbonate exchange; muscle contraction	↓ 0.77	↑ 1.33

Two genes in particular stood out from this list because of their previous links to muscle functionality. Ppargc1b was markedly down-regulated in both Med12 microarrays, and PGC-1β cardiac-specific knockouts have been reported to display dysregulated gene sets involving Ca^{2+} signaling, glucocorticoid receptor signaling, ubiquinone biosynthesis, and mitochondrial dysfunction (Gurung et al., 2011). In addition to Ppargc1b, Ldb3 also is worthy of a deeper look. Ldb3 encodes the protein CYPHER/ZASP, shown to be involved in both heart and skeletal muscle function. Mutations in the Ldb3 gene have been associated with myofibrillar myopathy, ARVC, and dilated cardiomyopathy (Li et al., 2010; Strach et al., 2012). Cypher/ZASP is a

member of the PDZ-LIM domain protein family, demonstrated as a sarcomeric protein to play an essential role in sarcomeric integrity especially under contraction force stress (Cheng et al., 2011; Lin et al., 2013; Zhou et al., 2001). Thus, further study into the role of Med12 specifically in Ldb3 regulation is warranted.

Heart failure (HF) afflicts an estimated 5.8 million Americans each year, and over 23 million people worldwide, and the lifetime risk of developing HF has become one in five (Adams, 2001; Bui et al., 2011; Spudich, 2001). There is a major need for new therapies to repair or reverse severe forms of cardiac dysfunction and pathological remodeling associated with HF. Typically, heart failure is the final culmination of prolonged disease states accompanied by underlying hypertension, valvular insufficiency, ischemia, atherosclerosis, myocarditis, or mutations in genes encoding sarcomeric proteins (Adams, 2001). Given these diverse etiologies, it is not surprising that the final phenotypic manifestations of heart failure can also vary considerably, although dilated cardiomyopathy is the most common. This syndrome is characterized by a progressive loss in contractility and ejection fraction, ventricular chamber dilatation, and ventricular wall thinning. Correct regulation of troponin and myosin contractile protein gene isoforms is a critical determinant of not only cardiac but also skeletal striated muscle development and function, with misexpression frequently associated with impaired contractility or myopathies. Dilated cardiomyopathy is characterized by left ventricular enlargement, which increases diastolic dimension. Decrease in systolic function is also common, measured in terms of reduced fractional shortening. Though many genetic

factors have been associated with cardiomyopathies, it is estimated that they only account for approximately 40% of known cases (Hershberger et al., 2013).

Our studies allow for comparison of the transcriptomes of Med13 and Med12 deletion in cardiac tissue, as well as Med12 deletion in both striated muscle tissues, and suggest different functions for the kinase module subunits in each condition. However, no identical experiments could be conducted on each subunit mutant due to the high phenotypic disparity that would ultimately confound direct comparison. In order to overcome the lethality associated with embryonic deletion of MED12, studies utilizing inducible cardiac-specific or skeletal muscle-specific ablation of Med12 expression in the adult will be informative of its role in striated muscle function, post-development. Genetic studies in mice have shown that an increase in slow muscle fibers confers resistance to musculoskeletal and metabolic disease. In the future, we plan to study the effects of induced Med12 deletion in adult cardiac and skeletal muscles on the pathogenesis of type II diabetes induced hyperglycemia and obesity. Perhaps post-sexual maturity, the Med12 mutants mimic Med13 genetic manipulation in the context of metabolism.

These results suggest a significant role for the Mediator kinase submodule regulatory axis in the complex structure and function of striated muscle. As CDK8 and cyclin C reside in the kinase submodule along with MED12 and MED13, we intend in our future studies to also examine the roles of these subunits in the context of striated muscle. Additionally, MED12L, the MED12 paralog, is thought to act as MED12 within a separate composition of the Mediator complex. However, very little is known about the

function of this subunit.(Vogl et al., 2013). We are also interested in investigating the role of this alternative subunit in striated muscle.

As with the complexity of transcriptional programs and metabolic pathways, it is likely that Mediator complex composition remains not yet fully described to date. Novel putative paralogs and alternative isoforms of subunits are being discovered and studied currently, and more are suspected to exist based on bioinformatic studies. With MED12 and MED13 recently uncovered as important regulators of biological functions, it will be interesting to delve further into the many functional roles of specific Mediator subunits.

APPENDIX A

QPCR PRIMER LIST

Med12-Exons 8/9
5’ – CCACTTGACCACCTGCCTAT
3’ – AGCGAACCTCAACTGCTTGT

Med12-Exons 12/13
5’ – TCCTAGTGCACCCATTTTCC
3’ – CTTTCACTTCGGGGATCAG

Axin2
5’ – ACTGACCGACGATTCCATGT
3’ - TGCATCTCTCTCTGGAGCTG

Ppargc1b
5’ – GAGGGCTCCGGCACTTC
3’ – CGTACTTGCTTTTCCCAGATGA

Ampd1
5’ – TCCCAGCCACAATGCCTCTA
3’ – TGCCGACCTCCCTCATCTTT

Lmna
5’ – GGGTCTTTCCGGAACTCCT
3’ – ACAAGTCCCCCTCCTTCTTG

CDK8
5’ – CAGATCCCATATCCCAAACG
3’ – GCCAGTTCCGTTAGTGTGGT

REFERENCES

Adams, K.F., Jr. (2001). New epidemiologic perspectives concerning mild-to-moderate heart failure. The American journal of medicine *110 Suppl 7A*, 6S-13S.

Agah, R., Frenkel, P.A., French, B.A., Michael, L.H., Overbeek, P.A., and Schneider, M.D. (1997). Gene recombination in postmitotic cells. Targeted expression of Cre recombinase provokes cardiac-restricted, site-specific rearrangement in adult ventricular muscle in vivo. The Journal of clinical investigation *100*, 169-179.

Agostini, M., Schoenmakers, E., Mitchell, C., Szatmari, I., Savage, D., Smith, A., Rajanayagam, O., Semple, R., Luan, J., Bath, L.*, et al.* (2006). Non-DNA binding, dominant-negative, human PPARgamma mutations cause lipodystrophic insulin resistance. Cell metabolism *4*, 303-311.

Alcalai, R., Seidman, J.G., and Seidman, C.E. (2008). Genetic basis of hypertrophic cardiomyopathy: from bench to the clinics. Journal of cardiovascular electrophysiology *19*, 104-110.

Allen, D.L., Harrison, B.C., Maass, A., Bell, M.L., Byrnes, W.C., and Leinwand, L.A. (2001). Cardiac and skeletal muscle adaptations to voluntary wheel running in the mouse. Journal of applied physiology *90*, 1900-1908.

Anderson, G.W., Zhu, Q., Metkowski, J., Stack, M.J., Gopinath, S., and Mariash, C.N. (2009). The Thrsp null mouse (Thrsp(tm1cnm)) and diet-induced obesity. Molecular and cellular endocrinology *302*, 99-107.

Arany, Z., He, H., Lin, J., Hoyer, K., Handschin, C., Toka, O., Ahmad, F., Matsui, T., Chin, S., Wu, P.H.*, et al.* (2005). Transcriptional coactivator PGC-1 alpha controls the energy state and contractile function of cardiac muscle. Cell metabolism *1*, 259-271.

Asadollahi, R., Oneda, B., Sheth, F., Azzarello-Burri, S., Baldinger, R., Joset, P., Latal, B., Knirsch, W., Desai, S., Baumer, A.*, et al.* (2013). Dosage changes of MED13L further delineate its role in congenital heart defects and intellectual disability. European journal of human genetics : EJHG *21*, 1100-1104.

Balaban, R.S., Kantor, H.L., Katz, L.A., and Briggs, R.W. (1986). Relation between work and phosphate metabolite in the in vivo paced mammalian heart. Science *232*, 1121-1123.

Bandman, E. (1992). Contractile protein isoforms in muscle development. Developmental biology *154*, 273-283.

Baskin, K.K., Grueter, C.E., Kusminski, C.M., Holland, W.L., Bookout, A.L., Satapati, S., Kong, Y.M., Burgess, S.C., Malloy, C.R., Scherer, P.E*., et al.* (2014). MED13-dependent signaling from the heart confers leanness by enhancing metabolism in adipose tissue and liver. EMBO molecular medicine *6*, 1610-1621.

Belakavadi, M., and Fondell, J.D. (2010). Cyclin-dependent kinase 8 positively cooperates with Mediator to promote thyroid hormone receptor-dependent transcriptional activation. Molecular and cellular biology *30*, 2437-2448.

Bottinelli, R., Schiaffino, S., and Reggiani, C. (1991). Force-velocity relations and myosin heavy chain isoform compositions of skinned fibres from rat skeletal muscle. The Journal of physiology *437*, 655-672.

Boutry-Kryza, N., Labalme, A., Till, M., Schluth-Bolard, C., Langue, J., Turleau, C., Edery, P., and Sanlaville, D. (2012). An 800 kb deletion at 17q23.2 including the MED13 (THRAP1) gene, revealed by aCGH in a patient with a SMC 17p. American journal of medical genetics Part A *158A*, 400-405.

Bui, A.L., Horwich, T.B., and Fonarow, G.C. (2011). Epidemiology and risk profile of heart failure. Nature reviews Cardiology *8*, 30-41.

Carvajal, K., and Moreno-Sanchez, R. (2003). Heart metabolic disturbances in cardiovascular diseases. Archives of medical research *34*, 89-99.

Casamassimi, A., and Napoli, C. (2007). Mediator complexes and eukaryotic transcription regulation: an overview. Biochimie *89*, 1439-1446.

Chen, W., Zhang, X., Birsoy, K., and Roeder, R.G. (2010). A muscle-specific knockout implicates nuclear receptor coactivator MED1 in the regulation of glucose and

energy metabolism. Proceedings of the National Academy of Sciences of the United States of America *107*, 10196-10201.

Cheng, H., Zheng, M., Peter, A.K., Kimura, K., Li, X., Ouyang, K., Shen, T., Cui, L., Frank, D., Dalton, N.D*., et al.* (2011). Selective deletion of long but not short Cypher isoforms leads to late-onset dilated cardiomyopathy. Human molecular genetics *20*, 1751-1762.

Clark, R.D., Graham, J.M., Jr., Friez, M.J., Hoo, J.J., Jones, K.L., McKeown, C., Moeschler, J.B., Raymond, F.L., Rogers, R.C., Schwartz, C.E*., et al.* (2009). FG syndrome, an X-linked multiple congenital anomaly syndrome: the clinical phenotype and an algorithm for diagnostic testing. Genetics in medicine : official journal of the American College of Medical Genetics *11*, 769-775.

Conaway, R.C., and Conaway, J.W. (2011). Function and regulation of the Mediator complex. Current opinion in genetics & development *21*, 225-230.

Conaway, R.C., and Conaway, J.W. (2013). The Mediator complex and transcription elongation. Biochimica et biophysica acta *1829*, 69-75.

Crabtree, G.R., and Olson, E.N. (2002). NFAT signaling: choreographing the social lives of cells. Cell *109 Suppl*, S67-79.

Crunkhorn, S., and Patti, M.E. (2008). Links between thyroid hormone action, oxidative metabolism, and diabetes risk? Thyroid : official journal of the American Thyroid Association *18*, 227-237.

Czubryt, M.P., McAnally, J., Fishman, G.I., and Olson, E.N. (2003). Regulation of peroxisome proliferator-activated receptor gamma coactivator 1 alpha (PGC-1 alpha) and mitochondrial function by MEF2 and HDAC5. Proceedings of the National Academy of Sciences of the United States of America *100*, 1711-1716.

Donner, A.J., Szostek, S., Hoover, J.M., and Espinosa, J.M. (2007). CDK8 is a stimulus-specific positive coregulator of p53 target genes. Molecular cell *27*, 121-133.

Finck, B.N., and Kelly, D.P. (2006). PGC-1 coactivators: inducible regulators of energy metabolism in health and disease. The Journal of clinical investigation *116*, 615-622.

Finck, B.N., and Kelly, D.P. (2007). Peroxisome proliferator-activated receptor gamma coactivator-1 (PGC-1) regulatory cascade in cardiac physiology and disease. Circulation *115*, 2540-2548.

Finck, B.N., Lehman, J.J., Leone, T.C., Welch, M.J., Bennett, M.J., Kovacs, A., Han, X., Gross, R.W., Kozak, R., Lopaschuk, G.D.*, et al.* (2002). The cardiac phenotype induced by PPARalpha overexpression mimics that caused by diabetes mellitus. The Journal of clinical investigation *109*, 121-130.

Firestein, R., Bass, A.J., Kim, S.Y., Dunn, I.F., Silver, S.J., Guney, I., Freed, E., Ligon, A.H., Vena, N., Ogino, S.*, et al.* (2008). CDK8 is a colorectal cancer oncogene that regulates beta-catenin activity. Nature *455*, 547-551.

Fondell, J.D., Guermah, M., Malik, S., and Roeder, R.G. (1999). Thyroid hormone receptor-associated proteins and general positive cofactors mediate thyroid hormone receptor function in the absence of the TATA box-binding protein-associated factors of TFIID. Proceedings of the National Academy of Sciences of the United States of America *96*, 1959-1964.

Ge, K., Guermah, M., Yuan, C.X., Ito, M., Wallberg, A.E., Spiegelman, B.M., and Roeder, R.G. (2002). Transcription coactivator TRAP220 is required for PPAR gamma 2-stimulated adipogenesis. Nature *417*, 563-567.

Geiger, P.C., Cody, M.J., and Sieck, G.C. (1999). Force-calcium relationship depends on myosin heavy chain and troponin isoforms in rat diaphragm muscle fibers. Journal of applied physiology *87*, 1894-1900.

Go, A.S., Mozaffarian, D., Roger, V.L., Benjamin, E.J., Berry, J.D., Borden, W.B., Bravata, D.M., Dai, S., Ford, E.S., Fox, C.S.*, et al.* (2013). Heart disease and stroke statistics--2013 update: a report from the American Heart Association. Circulation *127*, e6-e245.

Graham, J.M., Jr., and Schwartz, C.E. (2013). MED12 related disorders. American journal of medical genetics Part A *161A*, 2734-2740.

Grueter, C.E., van Rooij, E., Johnson, B.A., DeLeon, S.M., Sutherland, L.B., Qi, X., Gautron, L., Elmquist, J.K., Bassel-Duby, R., and Olson, E.N. (2012). A cardiac microRNA governs systemic energy homeostasis by regulation of MED13. Cell *149*, 671-683.

Gurung, I.S., Medina-Gomez, G., Kis, A., Baker, M., Velagapudi, V., Neogi, S.G., Campbell, M., Rodriguez-Cuenca, S., Lelliott, C., McFarlane, I.*, et al.* (2011). Deletion of the metabolic transcriptional coactivator PGC1beta induces cardiac arrhythmia. Cardiovascular research *92*, 29-38.

Harmancey, R., Wilson, C.R., and Taegtmeyer, H. (2008). Adaptation and maladaptation of the heart in obesity. Hypertension *52*, 181-187.

Heron-Milhavet, L., Mamaeva, D., LeRoith, D., Lamb, N.J., and Fernandez, A. (2010). Impaired muscle regeneration and myoblast differentiation in mice with a muscle-specific KO of IGF-IR. Journal of cellular physiology *225*, 1-6.

Hershberger, R.E., Hedges, D.J., and Morales, A. (2013). Dilated cardiomyopathy: the complexity of a diverse genetic architecture. Nature reviews Cardiology *10*, 531-547.

Hong, S.K., Haldin, C.E., Lawson, N.D., Weinstein, B.M., Dawid, I.B., and Hukriede, N.A. (2005). The zebrafish kohtalo/trap230 gene is required for the development of the brain, neural crest, and pronephric kidney. Proceedings of the National Academy of Sciences of the United States of America *102*, 18473-18478.

Huang, Y., Li, W., Yao, X., Lin, Q.J., Yin, J.W., Liang, Y., Heiner, M., Tian, B., Hui, J., and Wang, G. (2012). Mediator complex regulates alternative mRNA processing via the MED23 subunit. Molecular cell *45*, 459-469.

Huss, J.M., and Kelly, D.P. (2004). Nuclear receptor signaling and cardiac energetics. Circulation research *95*, 568-578.

Ito, M., and Roeder, R.G. (2001). The TRAP/SMCC/Mediator complex and thyroid hormone receptor function. Trends in endocrinology and metabolism: TEM *12*, 127-134.

Ito, M., Yuan, C.X., Okano, H.J., Darnell, R.B., and Roeder, R.G. (2000). Involvement of the TRAP220 component of the TRAP/SMCC coactivator complex in embryonic development and thyroid hormone action. Molecular cell *5*, 683-693.

Janody, F., Martirosyan, Z., Benlali, A., and Treisman, J.E. (2003). Two subunits of the Drosophila mediator complex act together to control cell affinity. Development *130*, 3691-3701.

Jia, Y., Viswakarma, N., and Reddy, J.K. (2014). Med1 subunit of the mediator complex in nuclear receptor-regulated energy metabolism, liver regeneration, and hepatocarcinogenesis. Gene expression *16*, 63-75.

Jones, J.R., Barrick, C., Kim, K.A., Lindner, J., Blondeau, B., Fujimoto, Y., Shiota, M., Kesterson, R.A., Kahn, B.B., and Magnuson, M.A. (2005). Deletion of PPARgamma in adipose tissues of mice protects against high fat diet-induced obesity and insulin resistance. Proceedings of the National Academy of Sciences of the United States of America *102*, 6207-6212.

Kagey, M.H., Newman, J.J., Bilodeau, S., Zhan, Y., Orlando, D.A., van Berkum, N.L., Ebmeier, C.C., Goossens, J., Rahl, P.B., Levine, S.S.*, et al.* (2010). Mediator and cohesin connect gene expression and chromatin architecture. Nature *467*, 430-435.

Knuesel, M.T., Meyer, K.D., Bernecky, C., and Taatjes, D.J. (2009a). The human CDK8 subcomplex is a molecular switch that controls Mediator coactivator function. Genes & development *23*, 439-451.

Knuesel, M.T., Meyer, K.D., Donner, A.J., Espinosa, J.M., and Taatjes, D.J. (2009b). The human CDK8 subcomplex is a histone kinase that requires Med12 for activity and can function independently of mediator. Molecular and cellular biology *29*, 650-661.

Krebs, P., Fan, W., Chen, Y.H., Tobita, K., Downes, M.R., Wood, M.R., Sun, L., Li, X., Xia, Y., Ding, N.*, et al.* (2011). Lethal mitochondrial cardiomyopathy in a hypomorphic Med30 mouse mutant is ameliorated by ketogenic diet. Proceedings of the National Academy of Sciences of the United States of America *108*, 19678-19682.

Kuo, I.Y., and Ehrlich, B.E. (2015). Signaling in Muscle Contraction. Cold Spring Harbor perspectives in biology *7*.

Lee, J.H., Bassel-Duby, R., and Olson, E.N. (2014). Heart- and muscle-derived signaling system dependent on MED13 and Wingless controls obesity in Drosophila. Proceedings of the National Academy of Sciences of the United States of America *111*, 9491-9496.

Lehman, W., Craig, R., and Vibert, P. (1994). Ca(2+)-induced tropomyosin movement in Limulus thin filaments revealed by three-dimensional reconstruction. Nature *368*, 65-67.

Leone, T.C., Lehman, J.J., Finck, B.N., Schaeffer, P.J., Wende, A.R., Boudina, S., Courtois, M., Wozniak, D.F., Sambandam, N., Bernal-Mizrachi, C*., et al.* (2005). PGC-1alpha deficiency causes multi-system energy metabolic derangements: muscle dysfunction, abnormal weight control and hepatic steatosis. PLoS biology *3*, e101.

Li, S., Czubryt, M.P., McAnally, J., Bassel-Duby, R., Richardson, J.A., Wiebel, F.F., Nordheim, A., and Olson, E.N. (2005). Requirement for serum response factor for skeletal muscle growth and maturation revealed by tissue-specific gene deletion in mice. Proceedings of the National Academy of Sciences of the United States of America *102*, 1082-1087.

Li, Z., Ai, T., Samani, K., Xi, Y., Tzeng, H.P., Xie, M., Wu, S., Ge, S., Taylor, M.D., Dong, J.W*., et al.* (2010). A ZASP missense mutation, S196L, leads to cytoskeletal and electrical abnormalities in a mouse model of cardiomyopathy. Circulation Arrhythmia and electrophysiology *3*, 646-656.

Lin, C., Guo, X., Lange, S., Liu, J., Ouyang, K., Yin, X., Jiang, L., Cai, Y., Mu, Y., Sheikh, F*., et al.* (2013). Cypher/ZASP is a novel A-kinase anchoring protein. The Journal of biological chemistry *288*, 29403-29413.

Lin, J., Handschin, C., and Spiegelman, B.M. (2005). Metabolic control through the PGC-1 family of transcription coactivators. Cell metabolism *1*, 361-370.

Lin, J., Wu, H., Tarr, P.T., Zhang, C.Y., Wu, Z., Boss, O., Michael, L.F., Puigserver, P., Isotani, E., Olson, E.N., *et al.* (2002). Transcriptional co-activator PGC-1 alpha drives the formation of slow-twitch muscle fibres. Nature *418*, 797-801.

Liu, X., Bushnell, D.A., and Kornberg, R.D. (2013). RNA polymerase II transcription: structure and mechanism. Biochimica et biophysica acta *1829*, 2-8.

Malik, S., Guermah, M., Yuan, C.X., Wu, W., Yamamura, S., and Roeder, R.G. (2004). Structural and functional organization of TRAP220, the TRAP/mediator subunit that is targeted by nuclear receptors. Molecular and cellular biology *24*, 8244-8254.

Malik, S., and Roeder, R.G. (2010). The metazoan Mediator co-activator complex as an integrative hub for transcriptional regulation. Nature reviews Genetics *11*, 761-772.

Maron, B.J., Gardin, J.M., Flack, J.M., Gidding, S.S., Kurosaki, T.T., and Bild, D.E. (1995). Prevalence of hypertrophic cardiomyopathy in a general population of young adults. Echocardiographic analysis of 4111 subjects in the CARDIA Study. Coronary Artery Risk Development in (Young) Adults. Circulation *92*, 785-789.

Matsuzaka, T., Shimano, H., Yahagi, N., Kato, T., Atsumi, A., Yamamoto, T., Inoue, N., Ishikawa, M., Okada, S., Ishigaki, N., *et al.* (2007). Crucial role of a long-chain fatty acid elongase, Elovl6, in obesity-induced insulin resistance. Nature medicine *13*, 1193-1202.

Mavalli, M.D., DiGirolamo, D.J., Fan, Y., Riddle, R.C., Campbell, K.S., van Groen, T., Frank, S.J., Sperling, M.A., Esser, K.A., Bamman, M.M., *et al.* (2010). Distinct growth hormone receptor signaling modes regulate skeletal muscle development and insulin sensitivity in mice. The Journal of clinical investigation *120*, 4007-4020.

McRae, A.T., 3rd, Chung, M.K., and Asher, C.R. (2001). Arrhythmogenic right ventricular cardiomyopathy: a cause of sudden death in young people. Cleveland Clinic journal of medicine *68*, 459-467.

Mitchell, C.S., Savage, D.B., Dufour, S., Schoenmakers, N., Murgatroyd, P., Befroy, D., Halsall, D., Northcott, S., Raymond-Barker, P., Curran, S., *et al.* (2010).

Resistance to thyroid hormone is associated with raised energy expenditure, muscle mitochondrial uncoupling, and hyperphagia. The Journal of clinical investigation *120*, 1345-1354.

Montgomery, R.L., Hullinger, T.G., Semus, H.M., Dickinson, B.A., Seto, A.G., Lynch, J.M., Stack, C., Latimer, P.A., Olson, E.N., and van Rooij, E. (2011). Therapeutic inhibition of miR-208a improves cardiac function and survival during heart failure. Circulation *124*, 1537-1547.

Mukundan, B., and Ansari, A. (2011). Novel role for mediator complex subunit Srb5/Med18 in termination of transcription. The Journal of biological chemistry *286*, 37053-37057.

Muncke, N., Jung, C., Rudiger, H., Ulmer, H., Roeth, R., Hubert, A., Goldmuntz, E., Driscoll, D., Goodship, J., Schon, K.*, et al.* (2003). Missense mutations and gene interruption in PROSIT240, a novel TRAP240-like gene, in patients with congenital heart defect (transposition of the great arteries). Circulation *108*, 2843-2850.

Napoli, C., Sessa, M., Infante, T., and Casamassimi, A. (2012). Unraveling framework of the ancestral Mediator complex in human diseases. Biochimie *94*, 579-587.

Naya, F.J., Mercer, B., Shelton, J., Richardson, J.A., Williams, R.S., and Olson, E.N. (2000). Stimulation of slow skeletal muscle fiber gene expression by calcineurin in vivo. The Journal of biological chemistry *275*, 4545-4548.

Niu, Z., Yu, W., Zhang, S.X., Barron, M., Belaguli, N.S., Schneider, M.D., Parmacek, M., Nordheim, A., and Schwartz, R.J. (2005). Conditional mutagenesis of the murine serum response factor gene blocks cardiogenesis and the transcription of downstream gene targets. The Journal of biological chemistry *280*, 32531-32538.

Ogilvie, R.W., and Feeback, D.L. (1990). A metachromatic dye-ATPase method for the simultaneous identification of skeletal muscle fiber types I, IIA, IIB and IIC. Stain technology *65*, 231-241.

Parlakian, A., Charvet, C., Escoubet, B., Mericskay, M., Molkentin, J.D., Gary-Bobo, G., De Windt, L.J., Ludosky, M.A., Paulin, D., Daegelen, D.*, et al.* (2005).

Temporally controlled onset of dilated cardiomyopathy through disruption of the SRF gene in adult heart. Circulation *112*, 2930-2939.

Parlakian, A., Tuil, D., Hamard, G., Tavernier, G., Hentzen, D., Concordet, J.P., Paulin, D., Li, Z., and Daegelen, D. (2004). Targeted inactivation of serum response factor in the developing heart results in myocardial defects and embryonic lethality. Molecular and cellular biology *24*, 5281-5289.

Pavri, R., Lewis, B., Kim, T.K., Dilworth, F.J., Erdjument-Bromage, H., Tempst, P., de Murcia, G., Evans, R., Chambon, P., and Reinberg, D. (2005). PARP-1 determines specificity in a retinoid signaling pathway via direct modulation of mediator. Molecular cell *18*, 83-96.

Pette, D., and Staron, R.S. (1997). Mammalian skeletal muscle fiber type transitions. International review of cytology *170*, 143-223.

Philibert, R., Caspers, K., Langbehn, D., Troughton, E.P., Yucuis, R., Sandhu, H.K., and Cadoret, R.J. (2002). The association of a HOPA polymorphism with major depression and phobia. Comprehensive psychiatry *43*, 404-410.

Pospisilik, J.A., Schramek, D., Schnidar, H., Cronin, S.J., Nehme, N.T., Zhang, X., Knauf, C., Cani, P.D., Aumayr, K., Todoric, J.*, et al.* (2010). Drosophila genome-wide obesity screen reveals hedgehog as a determinant of brown versus white adipose cell fate. Cell *140*, 148-160.

Rando, T.A., and Blau, H.M. (1997). Methods for myoblast transplantation. Methods in cell biology *52*, 261-272.

Rau, M.J., Fischer, S., and Neumann, C.J. (2006). Zebrafish Trap230/Med12 is required as a coactivator for Sox9-dependent neural crest, cartilage and ear development. Developmental biology *296*, 83-93.

Riehle, C., and Abel, E.D. (2012). PGC-1 proteins and heart failure. Trends in cardiovascular medicine *22*, 98-105.

Risheg, H., Graham, J.M., Jr., Clark, R.D., Rogers, R.C., Opitz, J.M., Moeschler, J.B., Peiffer, A.P., May, M., Joseph, S.M., Jones, J.R.*, et al.* (2007). A recurrent

mutation in MED12 leading to R961W causes Opitz-Kaveggia syndrome. Nature genetics *39*, 451-453.

Rocha, P.P., Bleiss, W., and Schrewe, H. (2010a). Mosaic expression of Med12 in female mice leads to exencephaly, spina bifida, and craniorachischisis. Birth defects research Part A, Clinical and molecular teratology *88*, 626-632.

Rocha, P.P., Scholze, M., Bleiss, W., and Schrewe, H. (2010b). Med12 is essential for early mouse development and for canonical Wnt and Wnt/PCP signaling. Development *137*, 2723-2731.

Rolfe, D.F., and Brown, G.C. (1997). Cellular energy utilization and molecular origin of standard metabolic rate in mammals. Physiological reviews *77*, 731-758.

Rommel, C., Bodine, S.C., Clarke, B.A., Rossman, R., Nunez, L., Stitt, T.N., Yancopoulos, G.D., and Glass, D.J. (2001). Mediation of IGF-1-induced skeletal myotube hypertrophy by PI(3)K/Akt/mTOR and PI(3)K/Akt/GSK3 pathways. Nature cell biology *3*, 1009-1013.

Rowe, G.C., Jiang, A., and Arany, Z. (2010). PGC-1 coactivators in cardiac development and disease. Circulation research *107*, 825-838.

Saffitz, J.E., and Yamada, K.A. (1998). Do alterations in intercellular coupling play a role in cardiac contractile dysfunction? Circulation *97*, 630-632.

Salvatore, D., Simonides, W.S., Dentice, M., Zavacki, A.M., and Larsen, P.R. (2014). Thyroid hormones and skeletal muscle--new insights and potential implications. Nature reviews Endocrinology *10*, 206-214.

Sanbe, A., Fewell, J.G., Gulick, J., Osinska, H., Lorenz, J., Hall, D.G., Murray, L.A., Kimball, T.R., Witt, S.A., and Robbins, J. (1999). Abnormal cardiac structure and function in mice expressing nonphosphorylatable cardiac regulatory myosin light chain 2. The Journal of biological chemistry *274*, 21085-21094.

Schiaffino, S., and Mammucari, C. (2011). Regulation of skeletal muscle growth by the IGF1-Akt/PKB pathway: insights from genetic models. Skeletal muscle *1*, 4.

Schiaffino, S., and Reggiani, C. (2011). Fiber types in mammalian skeletal muscles. Physiological reviews *91*, 1447-1531.

Schuler, M., Ali, F., Metzger, E., Chambon, P., and Metzger, D. (2005). Temporally controlled targeted somatic mutagenesis in skeletal muscles of the mouse. Genesis *41*, 165-170.

Schwartz, C.E., Tarpey, P.S., Lubs, H.A., Verloes, A., May, M.M., Risheg, H., Friez, M.J., Futreal, P.A., Edkins, S., Teague, J.*, et al.* (2007). The original Lujan syndrome family has a novel missense mutation (p.N1007S) in the MED12 gene. Journal of medical genetics *44*, 472-477.

Sengenes, C., Berlan, M., De Glisezinski, I., Lafontan, M., and Galitzky, J. (2000). Natriuretic peptides: a new lipolytic pathway in human adipocytes. FASEB journal : official publication of the Federation of American Societies for Experimental Biology *14*, 1345-1351.

Shelton, J.M., Lee, M.H., Richardson, J.A., and Patel, S.B. (2000). Microsomal triglyceride transfer protein expression during mouse development. Journal of lipid research *41*, 532-537.

Shin, C.H., Chung, W.S., Hong, S.K., Ober, E.A., Verkade, H., Field, H.A., Huisken, J., and Stainier, D.Y. (2008). Multiple roles for Med12 in vertebrate endoderm development. Developmental biology *317*, 467-479.

Song, Y., Yao, X., and Ying, H. (2011). Thyroid hormone action in metabolic regulation. Protein & cell *2*, 358-368.

Spaeth, J.M., Kim, N.H., and Boyer, T.G. (2011). Mediator and human disease. Seminars in cell & developmental biology *22*, 776-787.

Spudich, J.A. (2001). The myosin swinging cross-bridge model. Nature reviews Molecular cell biology *2*, 387-392.

Steimel, A., Suh, J., Hussainkhel, A., Deheshi, S., Grants, J.M., Zapf, R., Moerman, D.G., Taubert, S., and Hutter, H. (2013). The C. elegans CDK8 Mediator module

regulates axon guidance decisions in the ventral nerve cord and during dorsal axon navigation. Developmental biology *377*, 385-398.

Strach, K., Reimann, J., Thomas, D., Naehle, C.P., Kress, W., and Kornblum, C. (2012). ZASPopathy with childhood-onset distal myopathy. Journal of neurology *259*, 1494-1496.

Subramaniam, A., Jones, W.K., Gulick, J., Wert, S., Neumann, J., and Robbins, J. (1991). Tissue-specific regulation of the alpha-myosin heavy chain gene promoter in transgenic mice. The Journal of biological chemistry *266*, 24613-24620.

Templeton, G.H., Sweeney, H.L., Timson, B.F., Padalino, M., and Dudenhoeffer, G.A. (1988). Changes in fiber composition of soleus muscle during rat hindlimb suspension. Journal of applied physiology *65*, 1191-1195.

Thomas, P.D., Kejariwal, A., Guo, N., Mi, H., Campbell, M.J., Muruganujan, A., and Lazareva-Ulitsky, B. (2006). Applications for protein sequence-function evolution data: mRNA/protein expression analysis and coding SNP scoring tools. Nucleic acids research *34*, W645-650.

Treisman, J. (2001). Drosophila homologues of the transcriptional coactivation complex subunits TRAP240 and TRAP230 are required for identical processes in eye-antennal disc development. Development *128*, 603-615.

Van Gaal, L.F., Mertens, I.L., and De Block, C.E. (2006). Mechanisms linking obesity with cardiovascular disease. Nature *444*, 875-880.

van Rooij, E., Sutherland, L.B., Qi, X., Richardson, J.A., Hill, J., and Olson, E.N. (2007). Control of stress-dependent cardiac growth and gene expression by a microRNA. Science *316*, 575-579.

Vogl, M.R., Reiprich, S., Kuspert, M., Kosian, T., Schrewe, H., Nave, K.A., and Wegner, M. (2013). Sox10 cooperates with the mediator subunit 12 during terminal differentiation of myelinating glia. The Journal of neuroscience : the official journal of the Society for Neuroscience *33*, 6679-6690.

Wang, X., Yang, N., Uno, E., Roeder, R.G., and Guo, S. (2006). A subunit of the mediator complex regulates vertebrate neuronal development. Proceedings of the National Academy of Sciences of the United States of America *103*, 17284-17289.

Watanabe, M., Houten, S.M., Mataki, C., Christoffolete, M.A., Kim, B.W., Sato, H., Messaddeq, N., Harney, J.W., Ezaki, O., Kodama, T.*, et al.* (2006). Bile acids induce energy expenditure by promoting intracellular thyroid hormone activation. Nature *439*, 484-489.

Wolff, A.V., Niday, A.K., Voelker, K.A., Call, J.A., Evans, N.P., Granata, K.P., and Grange, R.W. (2006). Passive mechanical properties of maturing extensor digitorum longus are not affected by lack of dystrophin. Muscle & nerve *34*, 304-312.

Wu, Y., Li, Y., Lange, E.M., Croteau-Chonka, D.C., Kuzawa, C.W., McDade, T.W., Qin, L., Curocichin, G., Borja, J.B., Lange, L.A.*, et al.* (2010). Genome-wide association study for adiponectin levels in Filipino women identifies CDH13 and a novel uncommon haplotype at KNG1-ADIPOQ. Human molecular genetics *19*, 4955-4964.

Xu, W., and Ji, J.Y. (2011). Dysregulation of CDK8 and Cyclin C in tumorigenesis. Journal of genetics and genomics = Yi chuan xue bao *38*, 439-452.

Xu, Z.P., Wawrousek, E.F., and Piatigorsky, J. (2002). Transketolase haploinsufficiency reduces adipose tissue and female fertility in mice. Molecular and cellular biology *22*, 6142-6147.

Yang, F., Vought, B.W., Satterlee, J.S., Walker, A.K., Jim Sun, Z.Y., Watts, J.L., DeBeaumont, R., Saito, R.M., Hyberts, S.G., Yang, S.*, et al.* (2006). An ARC/Mediator subunit required for SREBP control of cholesterol and lipid homeostasis. Nature *442*, 700-704.

Yasui, K., Niwa, N., Takemura, H., Opthof, T., Muto, T., Horiba, M., Shimizu, A., Lee, J.K., Honjo, H., Kamiya, K.*, et al.* (2005). Pathophysiological significance of T-type Ca2+ channels: expression of T-type Ca2+ channels in fetal and diseased heart. Journal of pharmacological sciences *99*, 205-210.

Yin, J.W., and Wang, G. (2014). The Mediator complex: a master coordinator of transcription and cell lineage development. Development *141*, 977-987.

Zhou, Q., Chu, P.H., Huang, C., Cheng, C.F., Martone, M.E., Knoll, G., Shelton, G.D., Evans, S., and Chen, J. (2001). Ablation of Cypher, a PDZ-LIM domain Z-line protein, causes a severe form of congenital myopathy. The Journal of cell biology *155*, 605-612.

Zhou, Z., Yon Toh, S., Chen, Z., Guo, K., Ng, C.P., Ponniah, S., Lin, S.C., Hong, W., and Li, P. (2003). Cidea-deficient mice have lean phenotype and are resistant to obesity. Nature genetics *35*, 49-56.

Zhu, X., and Cheng, S.Y. (2010). New insights into regulation of lipid metabolism by thyroid hormone. Current opinion in endocrinology, diabetes, and obesity *17*, 408-413.

Zhu, X., Zhang, Y., Bjornsdottir, G., Liu, Z., Quan, A., Costanzo, M., Davila Lopez, M., Westholm, J.O., Ronne, H., Boone, C.*, et al.* (2011). Histone modifications influence mediator interactions with chromatin. Nucleic acids research *39*, 8342-8354.